

Multiscale analysis in image processing

Scale invariance in data processing

Barbara Pascal[†] and Nelly Pustelnik[‡]

bpascal-fr.github.io/talks

June 2025

[†] Nantes Université, École Centrale Nantes, CNRS, LS2N, F-44000 Nantes, France

[‡] CNRS, ENSL, Laboratoire de physique, F-69342 Lyon, France



FONDATION
SIMONE ET CINO
DEL DUCA
INSTITUT DE FRANCE

Self-similarity in signals and images

Self-similar fields

$\mathsf{F} : \mathbb{R}^d \rightarrow \mathbb{R}$ a random field is **self-similar** if there exists $H \in (0, 1)$ s.t.

$$(\forall c > 0) \quad \{\mathsf{F}(c\underline{x}); \underline{x} \in \mathbb{R}^N\} \stackrel{(d)}{=} c^H \{\mathsf{F}(\underline{x}); \underline{x} \in \mathbb{R}^d\}$$

with $\stackrel{(d)}{=}$ equality in distribution $\implies H$: **fractal** index

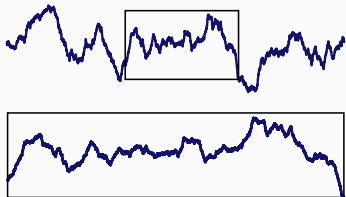
Self-similar fields

$\mathbf{F} : \mathbb{R}^d \rightarrow \mathbb{R}$ a random field is **self-similar** if there exists $H \in (0, 1)$ s.t.

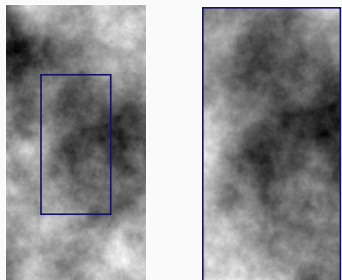
$$(\forall c > 0) \quad \{\mathbf{F}(c\underline{x}); \underline{x} \in \mathbb{R}^N\} \stackrel{(d)}{=} c^H \{\mathbf{F}(\underline{x}); \underline{x} \in \mathbb{R}^d\}$$

with $\stackrel{(d)}{=}$ equality in distribution $\implies H$: **fractal** index

Time series $\{\mathbf{F}(t), t \in \mathbb{R}\}$



Images $\mathbf{F} : \Omega \subset \mathbb{R}^2 \rightarrow \mathbb{R}$





BIARRITZ — Mai 1984 —

LES FRACTALES: OBJETS MATHÉMATIQUES,
MODÈLES PHYSIQUES ET CRÉATIONS ARTISTIQUES

Benoit B. MANDELBROT

IBM Thomas J. Watson Research Center, Yorktown Heights, NY, 10598, USA

RESUME

La géométrie fractale de la nature fut conçue et développée par l'auteur de ce travail et présentée pour la

The fractal geometry of nature was conceived and developed by the author, beginning in 1975. It started with

SUMMARY

"La géométrie fractal de la nature fut conçue et développée par l'auteur de ce travail et présentée pour la première fois en 1975. Ses sources se trouvent dans deux découvertes inattendues, aux multiples effets cumulatifs. Les fractales ont contribué à redonné (sic) aux mathématiques et à la physique un côté visuel et presque sensuel, et elles ont posé des questions nouvelles concernant l'esthétique et de nombreux problèmes d'informatique et d'infographie."

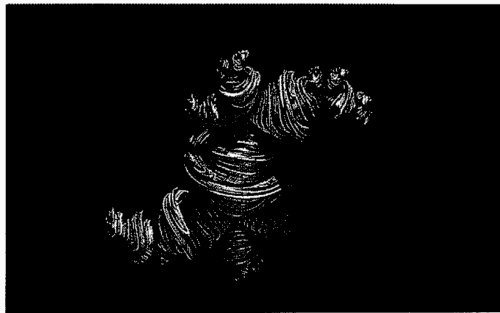


Figure 4 Dragon fractal quaternionique, réalisé par V. Alan Norton. Copyright 1983 by V. Alan Norton.

[B. B. Mandelbrot, 1983, "The fractal geometry of nature.", *W. H. Freeman and Co.*; B. B. Mandelbrot, 1984, *Colloque Images*]

Fractal objects in signal and image processing

- Physics: turbulent flows, geophysics [M. Nelkin, 1989, *J. Stat. Phys.*; B. Dubrulle, et al., 2022, *Philos. Trans. R. Soc. A.*]
- Financial forecasting [R.T. Baillie, ,1996, *J. Econom.*]
- Geography: relief representation, population in cities [L. Lucido, et al., 1998, *Int. J. Syst. Sci.*; J. Lengyel et al., 2025, *Sci. Rep.*]
- Cardiac activity mother-fetus [M. Doret et al., 2015, *PLoS One.*]
- Computer networks analysis, Internet traffic [J. Beran et al., 1995, *IEEE Trans. Commun.*; P. Abry, et al., 1998, *IEEE Trans. Inf. Theory*; R. Fontugne, et al., 2017, *IEEE/ACM Trans. Network.*]
- Infographics/computer graphics [J. L., Encarnação et al., 2012, *Springer Science & Business Media.*]

Isotropic texture segmentation

Intuition and examples of texture

Texture: periodically and/or stochastically repeated pattern.

Intuition and examples of texture

Texture: periodically and/or stochastically repeated pattern.



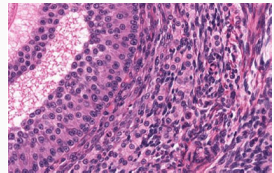
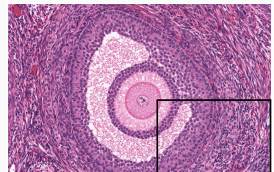
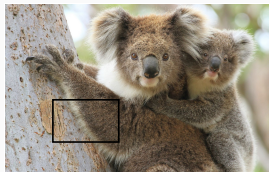
Intuition and examples of texture

Texture: periodically and/or stochastically repeated pattern.



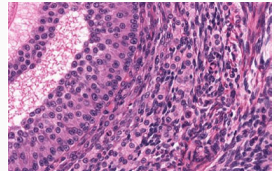
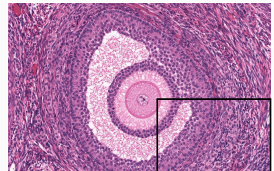
Intuition and examples of texture

Texture: periodically and/or stochastically repeated pattern.



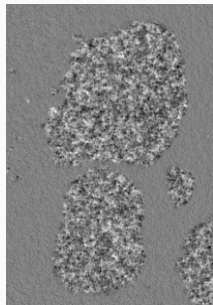
Intuition and examples of texture

Texture: periodically and/or stochastically repeated pattern.

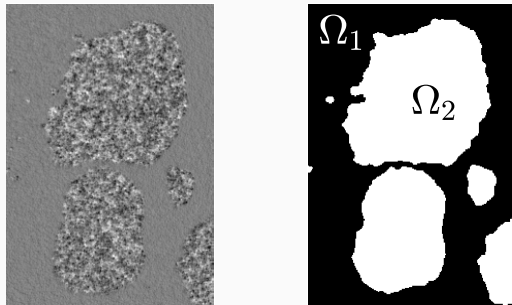


Crucial to describe and to process **real-world** images

Textured image segmentation



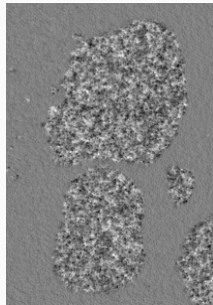
Textured image segmentation



Goal: obtain a partition of the image into L homogeneous textures

$$\Omega = \Omega_1 \sqcup \dots \sqcup \Omega_L$$

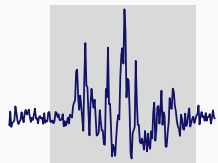
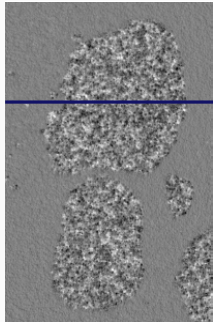
Textured image segmentation



Goal: obtain a partition of the image into L **homogeneous textures**

$$\Omega = \Omega_1 \sqcup \dots \sqcup \Omega_L$$

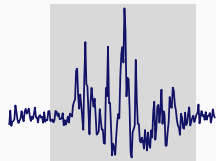
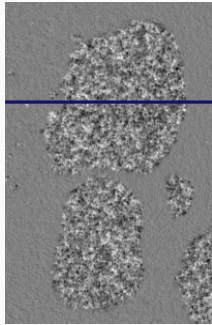
Features describing fractal textures



Features describing fractal textures

Fractals attributes

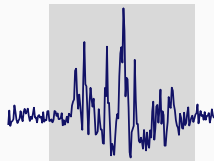
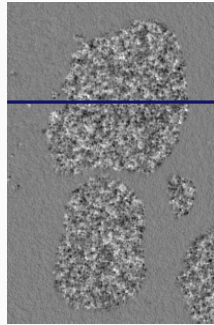
- variance σ^2 *amplitude of variations*



Features describing fractal textures

Fractals attributes

- variance σ^2 *amplitude of variations*
- local regularity h *scale invariance*

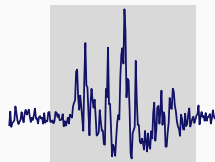
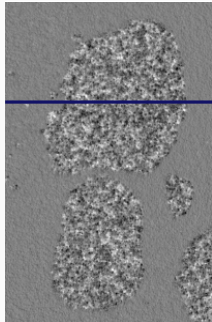


Features describing fractal textures

Fractals attributes

- variance σ^2 *amplitude of variations*
- local regularity h *scale invariance*

$$|f(\underline{x}) - f(\underline{y})| \leq \sigma(\underline{x}) |\underline{x} - \underline{y}|^{h(\underline{x})}$$

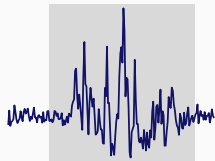
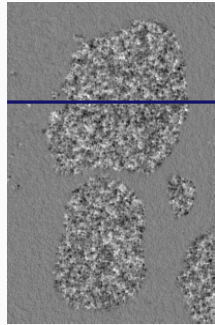
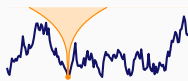
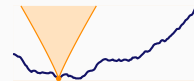


Features describing fractal textures

Fractals attributes

- variance σ^2 *amplitude of variations*
- local regularity h *scale invariance*

$$|f(\underline{x}) - f(\underline{y})| \leq \sigma(\underline{x}) |\underline{x} - \underline{y}|^{h(\underline{x})}$$

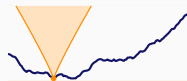


Features describing fractal textures

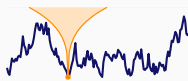
Fractals attributes

- variance σ^2 *amplitude of variations*
- local regularity h *scale invariance*

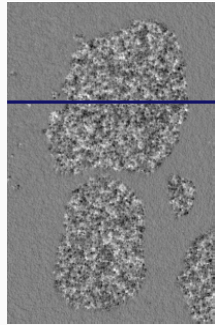
$$|f(\underline{x}) - f(\underline{y})| \leq \sigma(\underline{x}) |\underline{x} - \underline{y}|^{h(\underline{x})}$$



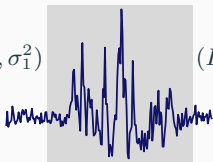
$$h(\underline{x}) \equiv H_1 = 0.9$$



$$h(\underline{x}) \equiv H_2 = 0.3$$



$$(H_2, \sigma_2^2)$$



$$(H_1, \sigma_1^2)$$

$$(H_1, \sigma_1^2)$$

Segmentation

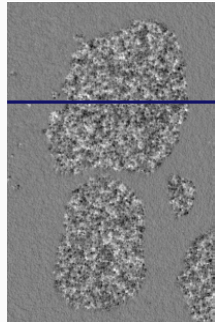
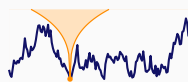
- h and σ^2 piecewise constant

Features describing fractal textures

Fractals attributes

- variance σ^2 *amplitude of variations*
- local regularity h *scale invariance*

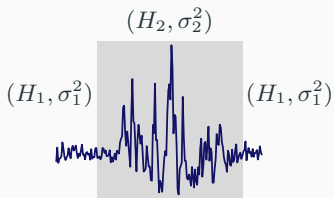
$$|f(\underline{x}) - f(\underline{y})| \leq \sigma(\underline{x}) |\underline{x} - \underline{y}|^{h(\underline{x})}$$



(H_2, σ_2^2)

Segmentation

- ▶ h and σ^2 piecewise constant
- ▶ region Ω_k characterized by (H_k, σ_k^2)



Self-similar Gaussian Fields: a few models

Let $H \in (0, 1)$ be a so-called **Hurst index**; $\sigma^2 > 0$ a variance;
 \tilde{W} the Fourier transform of a Wiener measure.

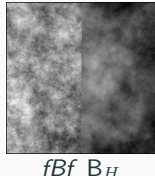
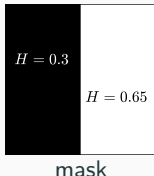
Self-similar Gaussian Fields: a few models

Let $H \in (0, 1)$ be a so-called **Hurst index**; $\sigma^2 > 0$ a variance;

\tilde{W} the Fourier transform of a Wiener measure.

- **Fractional Brownian Field** $B_H(\underline{x}) = \frac{\sigma}{\sqrt{C_H}} \int_{\mathbb{R}^2} \frac{e^{-i\langle \underline{x}, \underline{\xi} \rangle} - 1}{\|\underline{\xi}\|^{H+1}} \tilde{W}(d\underline{\xi})$

[B. B. Mandelbrot & J. W. Van Ness, 1968, *SIAM Rev.*]



Self-similar Gaussian Fields: a few models

Let $H \in (0, 1)$ be a so-called **Hurst index**; $\sigma^2 > 0$ a variance;

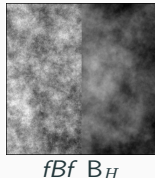
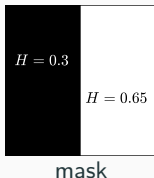
\tilde{W} the Fourier transform of a Wiener measure.

- **Fractional Brownian Field** $B_H(\underline{x}) = \frac{\sigma}{\sqrt{C_H}} \int_{\mathbb{R}^2} \frac{e^{-i\langle \underline{x}, \underline{\xi} \rangle} - 1}{\|\underline{\xi}\|^{H+1}} \tilde{W}(d\underline{\xi})$

[B. B. Mandelbrot & J. W. Van Ness, 1968, *SIAM Rev.*]

- **Fractional Gaussian Field** [B. Pascal et al., 2021, *Appl. Comp. Harmon. Anal.*]

$$G_H(\underline{x}) = \frac{1}{2} \underbrace{(B_H(\underline{x} + e_1) - B_H(\underline{x}))}_{\text{horizontal increment}} + \frac{1}{2} \underbrace{(B_H(\underline{x} + e_2) - B_H(\underline{x}))}_{\text{vertical increment}}$$



Self-similar Gaussian Fields: a few models

Let $H \in (0, 1)$ be a so-called **Hurst index**; $\sigma^2 > 0$ a variance;

\tilde{W} the Fourier transform of a Wiener measure.

- **Fractional Brownian Field** $B_H(\underline{x}) = \frac{\sigma}{\sqrt{C_H}} \int_{\mathbb{R}^2} \frac{e^{-i\langle \underline{x}, \underline{\xi} \rangle} - 1}{\|\underline{\xi}\|^{H+1}} \tilde{W}(d\underline{\xi})$

[B. B. Mandelbrot & J. W. Van Ness, 1968, *SIAM Rev.*]

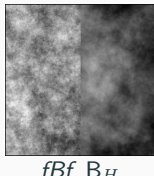
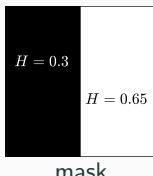
- **Fractional Gaussian Field** [B. Pascal et al., 2021, *Appl. Comp. Harmon. Anal.*]

$$G_H(\underline{x}) = \frac{1}{2} \underbrace{(B_H(\underline{x} + e_1) - B_H(\underline{x}))}_{\text{horizontal increment}} + \frac{1}{2} \underbrace{(B_H(\underline{x} + e_2) - B_H(\underline{x}))}_{\text{vertical increment}}$$

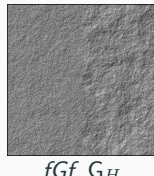
- **Filtered fBf**

[B. Pascal et al., 2025, *IEEE Stat. Signal Process.*]

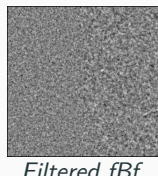
$$C_H(\underline{x}) = \langle B_H, w_{\underline{x}} \rangle, w \text{ isotropic high-pass filter}$$



fBf B_H



fGf G_H



Filtered fBf

Synthetic fractal textures for performance assessment

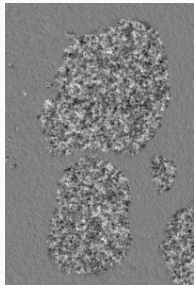
How to choose a model to generate synthetic textures?

Synthetic fractal textures for performance assessment

How to choose a model to generate synthetic textures?

- visually resemble real textures: isotropic, stationary

Real

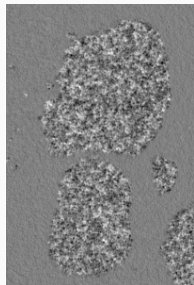


Synthetic fractal textures for performance assessment

How to choose a model to generate synthetic textures?

- visually resemble real textures: isotropic, stationary
- self-similar field characterized by (H, σ^2) such that $h(\underline{x}) \equiv H$

Real

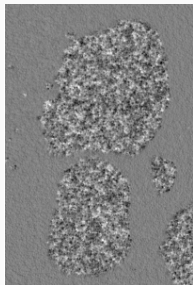


Synthetic fractal textures for performance assessment

How to choose a model to generate synthetic textures?

- visually resemble real textures: isotropic, stationary
- self-similar field characterized by (H, σ^2) such that $h(\underline{x}) \equiv H$
- easy to “patch”: no artifact at the border

Real



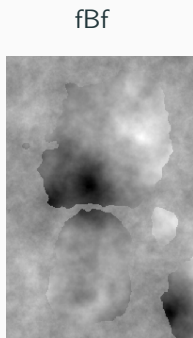
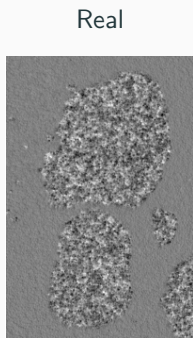
Mask



Synthetic fractal textures for performance assessment

How to choose a model to generate synthetic textures?

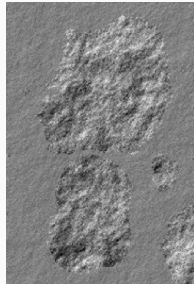
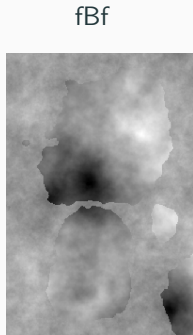
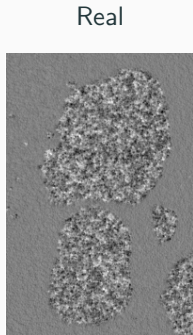
- visually resemble real textures: isotropic, stationary ✓
- self-similar field characterized by (H, σ^2) such that $h(\underline{x}) \equiv H$ ✓
- easy to “patch”: no artifact at the border ✗



Synthetic fractal textures for performance assessment

How to choose a model to generate synthetic textures?

- visually resemble real textures: isotropic, stationary ✓
- self-similar field characterized by (H, σ^2) such that $h(\underline{x}) \equiv H$ ✓
- easy to “patch”: no artifact at the border ✓



Multiscale analysis to probe local regularity

Field $X \in L^2(\mathbb{R}^2)$ and mother wavelet ψ with n_ψ **vanishing moments**

Proposition If the Hölder local regularity of F at \underline{x}_0 is $h(\underline{x}_0) \leq n_\psi$,

$$\exists A > 0, \quad |\mathcal{W}_f(\underline{x}, a)| \leq Aa^{h(\underline{x}_0)+1} \left(1 + \left\| \frac{\underline{x}_0 - \underline{x}}{a} \right\|^{h(\underline{x}_0)} \right)$$

[S. Jaffard, 1991, *Publicacions Matemàtiques*]

Multiscale analysis to probe local regularity

Field $X \in L^2(\mathbb{R}^2)$ and mother wavelet ψ with n_ψ **vanishing moments**

Proposition If the Hölder local regularity of F at \underline{x}_0 is $h(\underline{x}_0) \leq n_\psi$,

$$\exists A > 0, \quad |\mathcal{W}_f(\underline{x}, a)| \leq Aa^{h(\underline{x}_0)+1} \left(1 + \left\| \frac{\underline{x}_0 - \underline{x}}{a} \right\|^{h(\underline{x}_0)} \right)$$

[S. Jaffard, 1991, *Publicacions Matemàtiques*]

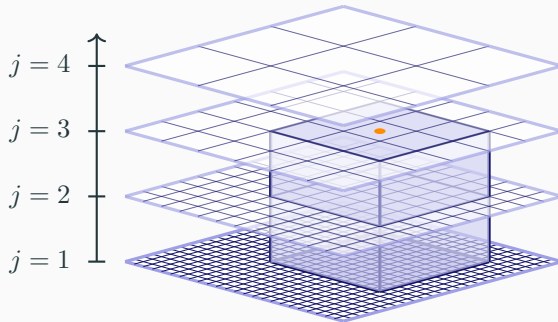
Discrete wavelet coefficients $\zeta_{j,\underline{k}} = \langle X, \psi_{j,\underline{k}} \rangle$ with ψ an L^1 -normalized

$$|\zeta_{j,\underline{k}}^{(m)}| \underset{2^j \rightarrow 0}{\lesssim} \eta(\underline{n}) 2^{jh(\underline{n})}, \quad \text{for } \underline{n} = 2^j \underline{k}$$

with $\eta(\underline{n})$ some positive-valued function

Decimated wavelet leader coefficients

$$\tilde{\mathcal{L}}_{j,\underline{k}}[\mathbf{X}] = \sup_{m=\{1,2,3\}} \left| 2^{j\gamma} \zeta_{j',\underline{k}'}^{(m)}[\mathbf{X}] \right|, \text{ with } \begin{cases} \lambda_{j,\underline{n}} = [\underline{k}2^j, (\underline{k}+1)2^j[\\ 3\lambda_{j,\underline{n}} = \bigcup_{\underline{p} \in \{-1,0,1\}^2} \lambda_{j,\underline{k}+\underline{p}}, \end{cases}$$
$$\lambda_{j',\underline{n}'} \subset 3\lambda_{j,\underline{n}}$$

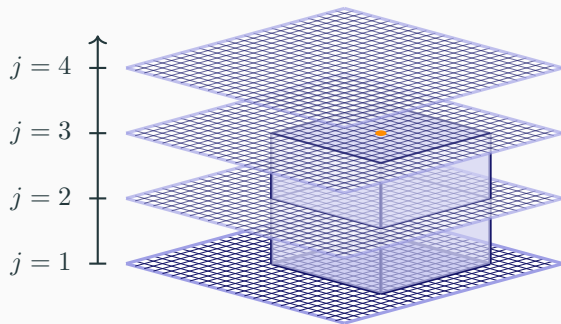


Wavelet p -Leader and Bootstrap based MultiFractal analysis (PLBMF)

irit.fr/~Herwig.Wendt/software

Undecimated wavelet leader coefficients

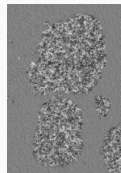
$$\mathcal{L}_{j,\underline{n}}[\mathbf{X}] = \sup_{m=\{1,2,3\}} \left| 2^{j\gamma} \zeta_{j',\underline{n}'}^{(m)}[\mathbf{X}] \right|, \text{ with } \begin{cases} \lambda_{j,\underline{n}} = [\underline{n}, \underline{n} + 2^j[\\ 3\lambda_{j,\underline{n}} = \bigcup_{\underline{p} \in \{-2^j, 0, 2^j\}^2} \lambda_{j,\underline{n}+\underline{p}}, \end{cases}$$
$$\lambda_{j',\underline{n}'} \subset 3\lambda_{j,\underline{n}}$$



[S. Jaffard, 2004, *Proc. Symp. Pure Math.*;
H. Wendt et al., 2008, *IEEE T. Signal Proces.*]

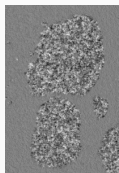
Multiscale analysis

Textured image



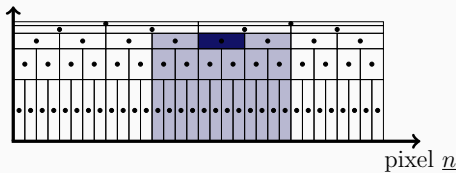
Multiscale analysis

Textured image



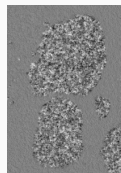
Local maximum of wavelet coefficients: $\mathcal{L}_{a,\cdot}$

scale a



Multiscale analysis

Textured image



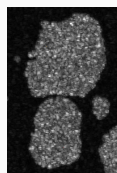
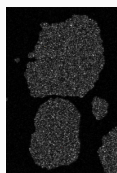
Local maximum of wavelet coefficients: $\mathcal{L}_{a,\cdot}$

Scale

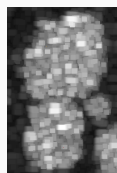
$a = 2^1$

$a = 2^2$

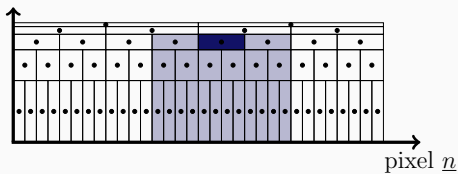
$a = 2^5$



...



scale a

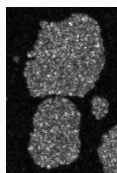
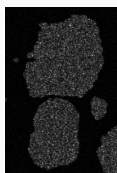
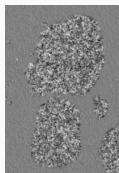


Multiscale analysis

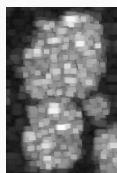
Textured image

Local maximum of wavelet coefficients: $\mathcal{L}_{a,\cdot}$

Scale $a = 2^1$ $a = 2^2$ $a = 2^5$



...



Proposition

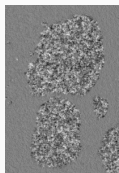
$$\log(\mathcal{L}_{a,\cdot}) \underset{a \rightarrow 0}{\simeq} \log(a) \frac{\text{h}}{\text{regularity}} + \frac{\text{v}}{\propto \log(\sigma^2)} \quad (\text{variance})$$

[S. Jaffard, 2004, *Proc. Symp. Pure Math.*;

H. Wendt et al., 2008, *IEEE T. Signal Proces.*]

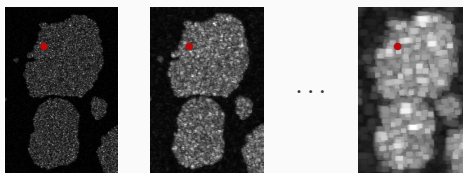
Multiscale analysis

Textured image



Local maximum of wavelet coefficients: $\mathcal{L}_{a,\cdot}$

Scale $a = 2^1$ $a = 2^2$ $a = 2^5$

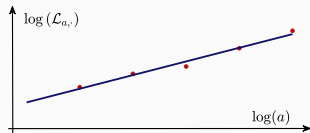


Proposition

$$\log(\mathcal{L}_{a,\cdot}) \underset{a \rightarrow 0}{\simeq} \log(a) \text{ regularity} + \frac{\text{v}}{\propto \log(\sigma^2)}$$

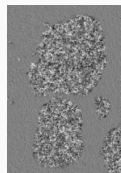
[S. Jaffard, 2004, *Proc. Symp. Pure Math.*;

H. Wendt et al., 2008, *IEEE T. Signal Proces.*]



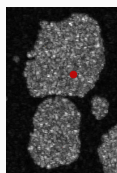
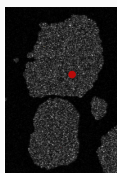
Multiscale analysis

Textured image

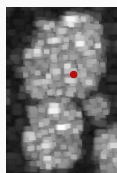


Local maximum of wavelet coefficients: $\mathcal{L}_{a,\cdot}$

Scale $a = 2^1$ $a = 2^2$ $a = 2^5$



...

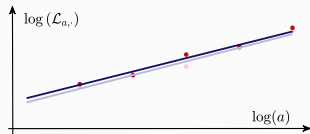


Proposition

$$\log(\mathcal{L}_{a,\cdot}) \underset{a \rightarrow 0}{\simeq} \log(a) \text{ regularity} + \frac{v}{\propto \log(\sigma^2)}$$

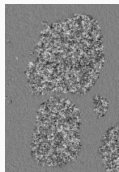
[S. Jaffard, 2004, *Proc. Symp. Pure Math.*;

H. Wendt et al., 2008, *IEEE T. Signal Proces.*]



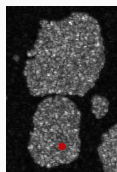
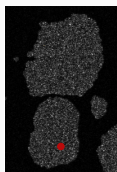
Multiscale analysis

Textured image

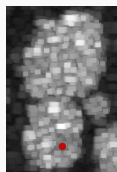


Local maximum of wavelet coefficients: $\mathcal{L}_{a,\cdot}$

Scale $a = 2^1$ $a = 2^2$ $a = 2^5$



...

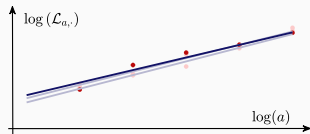


Proposition

$$\log(\mathcal{L}_{a,\cdot}) \underset{a \rightarrow 0}{\simeq} \log(a) \text{ regularity} + \frac{\text{v}}{\propto \log(\sigma^2)}$$

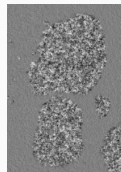
[S. Jaffard, 2004, *Proc. Symp. Pure Math.*;

H. Wendt et al., 2008, *IEEE T. Signal Proces.*]



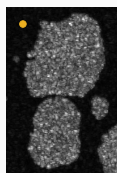
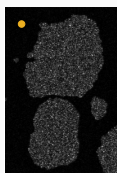
Multiscale analysis

Textured image

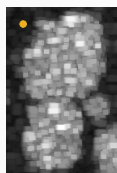


Local maximum of wavelet coefficients: $\mathcal{L}_{a,\cdot}$

Scale $a = 2^1$ $a = 2^2$ $a = 2^5$



...

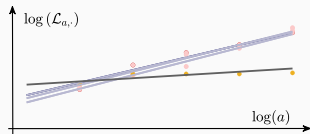


Proposition

$$\log(\mathcal{L}_{a,\cdot}) \underset{a \rightarrow 0}{\simeq} \log(a) \begin{matrix} \text{h} \\ \text{regularity} \end{matrix} + \begin{matrix} \text{v} \\ \propto \log(\sigma^2) \\ (\text{variance}) \end{matrix}$$

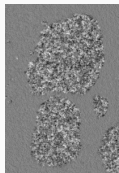
[S. Jaffard, 2004, *Proc. Symp. Pure Math.*;

H. Wendt et al., 2008, *IEEE T. Signal Proces.*]



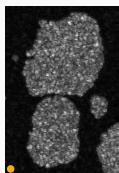
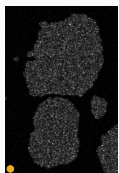
Multiscale analysis

Textured image

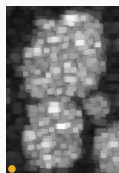


Local maximum of wavelet coefficients: $\mathcal{L}_{a,\cdot}$

Scale $a = 2^1$ $a = 2^2$ $a = 2^5$



...

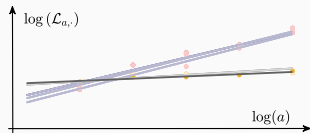


Proposition

$$\log(\mathcal{L}_{a,\cdot}) \underset{a \rightarrow 0}{\simeq} \log(a) \text{ regularity} + \frac{v}{\propto \log(\sigma^2)} \text{ (variance)}$$

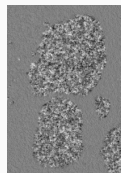
[S. Jaffard, 2004, *Proc. Symp. Pure Math.*;

H. Wendt et al., 2008, *IEEE T. Signal Proces.*]



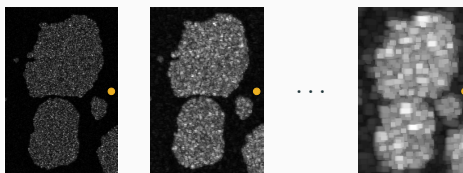
Multiscale analysis

Textured image



Local maximum of wavelet coefficients: $\mathcal{L}_{a,\cdot}$

Scale $a = 2^1$ $a = 2^2$ $a = 2^5$

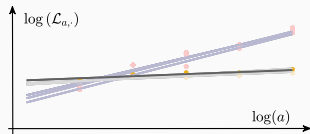


Proposition

$$\log(\mathcal{L}_{a,\cdot}) \underset{a \rightarrow 0}{\simeq} \log(a) \text{ regularity} + \frac{\text{v}}{\propto \log(\sigma^2)}$$

[S. Jaffard, 2004, *Proc. Symp. Pure Math.*;

H. Wendt et al., 2008, *IEEE T. Signal Proces.*]

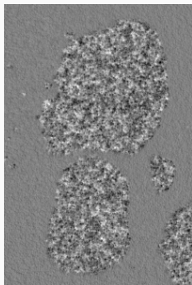


Direct punctual estimation

Linear regression

$$\log(\mathcal{L}_{a,\cdot}) \simeq \log(a)_{\text{regularity}} + \frac{h}{\alpha \log(\sigma^2)}$$

Textured image



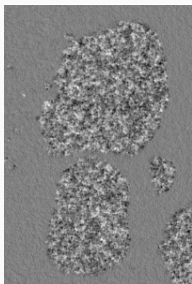
Direct punctual estimation

Linear regression

$$\log(\mathcal{L}_{a,\cdot}) \simeq \log(a) \frac{h}{\text{regularity}} + \frac{v}{\propto \log(\sigma^2)}$$

$$(\hat{h}^{\text{LR}}, \hat{v}^{\text{LR}}) = \underset{h,v}{\operatorname{argmin}} \sum_{a=a_{\min}}^{a_{\max}} \|\log(\mathcal{L}_{a,\cdot}) - \log(a)h - v\|^2$$

Textured image



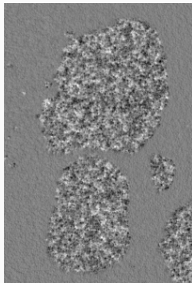
Direct punctual estimation

Linear regression

$$\log(\mathcal{L}_{a,\cdot}) \simeq \log(a) \frac{h}{\text{regularity}} + \frac{v}{\propto \log(\sigma^2)}$$

$$(\hat{h}^{\text{LR}}, \hat{v}^{\text{LR}}) = \underset{h, v}{\operatorname{argmin}} \sum_{a=a_{\min}}^{a_{\max}} \|\log(\mathcal{L}_{a,\cdot}) - \log(a)h - v\|^2$$

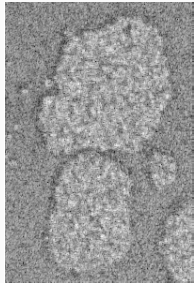
Textured image



Local regularity \hat{h}^{LR}



Local power \hat{v}^{LR}



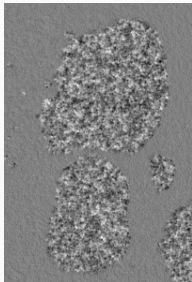
Direct punctual estimation

Linear regression

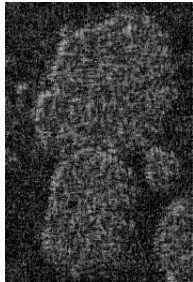
$$\mathbb{E} \log(\mathcal{L}_{a,\cdot}) = \log(a) \underset{\text{expected value}}{\bar{h}} + \underset{\propto \log(\sigma^2)}{\bar{v}}$$

$$(\hat{h}^{LR}, \hat{v}^{LR}) = \operatorname{argmin}_{h,v} \sum_{a=a_{\min}}^{a_{\max}} \|\log(\mathcal{L}_{a,\cdot}) - \log(a)h - v\|^2$$

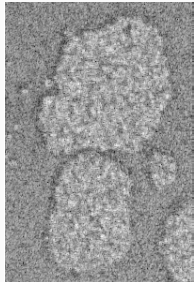
Textured image



Local regularity \hat{h}^{LR}



Local power \hat{v}^{LR}



A posteriori regularization

Linear regression \hat{h}^{LR}



A posteriori regularization

Finite differences $D_1 h$ (horizontal), $D_2 h$ (vertical) in each pixel

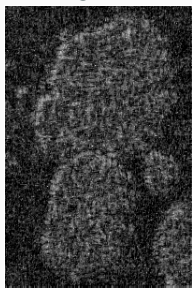
Linear regression \hat{h}^{LR}



A posteriori regularization

Finite differences $Dx = [D_1 h, D_2 h]$

Linear regression \hat{h}^{LR}



A posteriori regularization

Finite differences $Dx = [D_1 h, D_2 h]$

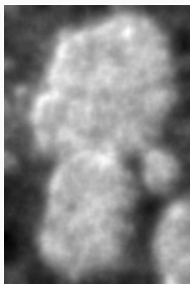
Filter smoothing (linear)

$$\begin{aligned} \operatorname{argmin}_h \|h - \hat{h}^{\text{LR}}\|^2 + \theta \|Dh\|_2^2 \\ = (I + \theta D^\top D)^{-1} \hat{h}^{\text{LR}} \end{aligned}$$

Linear regression \hat{h}^{LR}



Smoothing



A posteriori regularization

Finite differences $Dx = [D_1 h, D_2 h]$

Filter smoothing (linear)

$$\operatorname{argmin}_h \|h - \hat{h}^{\text{LR}}\|^2 + \theta \|Dh\|_2^2 \\ = (I + \theta D^\top D)^{-1} \hat{h}^{\text{LR}}$$

ROF denoising (nonlinear)

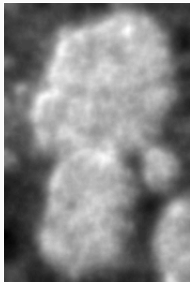
$$\operatorname{argmin}_h \|h - \hat{h}^{\text{LR}}\|^2 + \theta \|Dh\|_{2,1}$$

[F. Abboud et al., 2017, *J. Math. Imaging Vis.*]

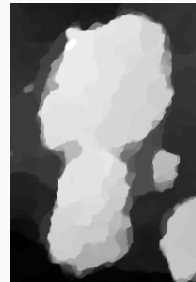
Linear regression \hat{h}^{LR}



Smoothing



ROF



A posteriori regularization

Finite differences $Dx = [D_1 h, D_2 h]$

Filter smoothing (linear)

$$\operatorname{argmin}_h \|h - \hat{h}^{\text{LR}}\|^2 + \theta \|Dh\|_2^2 \\ = (I + \theta D^\top D)^{-1} \hat{h}^{\text{LR}}$$

ROF denoising (nonlinear)

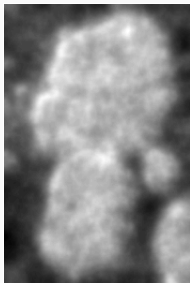
$$\operatorname{argmin}_h \|h - \hat{h}^{\text{LR}}\|^2 + \theta \|Dh\|_{2,1}$$

[F. Abboud et al., 2017, *J. Math. Imaging Vis.*]

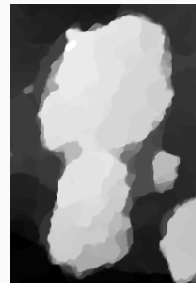
Linear regression \hat{h}^{LR}



Smoothing



ROF

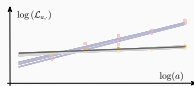


→ cumulative estimation variance and regularization bias

Functionals with either free or co-localized contours

$$\sum_a \frac{\|\log \mathcal{L}_{a,.} - \log(a)h - v\|^2}{\text{Least-Squares}}$$

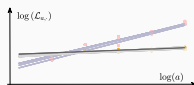
→ fidelity to the log-linear model



Functionals with either free or co-localized contours

$$\sum_a \frac{\|\log \mathcal{L}_{a,.} - \log(a)h - v\|^2}{\text{Least-Squares}} + \theta \frac{\mathcal{Q}(Dh, Dv; \alpha)}{\text{Total Variation}}$$

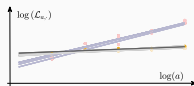
\rightarrow fidelity to the log-linear model
 \rightarrow favors piecewise constancy



Functionals with either free or co-localized contours

$$\underset{h,v}{\text{minimize}} \quad \sum_a \frac{\|\log \mathcal{L}_{a,.} - \log(a)h - v\|^2}{\text{Least-Squares}} + \theta \frac{\mathcal{Q}(Dh, Dv; \alpha)}{\text{Total Variation}}$$

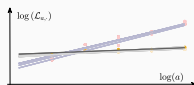
\rightarrow fidelity to the log-linear model
 \rightarrow favors piecewise constancy



Functionals with either free or co-localized contours

$$\underset{h,v}{\text{minimize}} \quad \sum_a \frac{\|\log \mathcal{L}_{a,.} - \log(a)h - v\|^2}{\text{Least-Squares}} + \theta \frac{\mathcal{Q}(Dh, Dv; \alpha)}{\text{Total Variation}}$$

\rightarrow fidelity to the log-linear model
 \rightarrow favors piecewise constancy

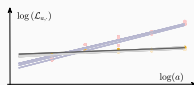


Finite differences $D_1 h$ (horizontal), $D_2 h$ (vertical) in each pixel

Functionals with either free or co-localized contours

$$\underset{h,v}{\text{minimize}} \quad \sum_a \frac{\|\log \mathcal{L}_{a,.} - \log(a)h - v\|^2}{\text{Least-Squares}} + \theta \frac{\mathcal{Q}(Dh, Dv; \alpha)}{\text{Total Variation}}$$

\rightarrow fidelity to the log-linear model
 \rightarrow favors piecewise constancy



Finite differences $Dh = [D_1 h, D_2 h]$

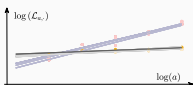
Free: h, v are **independently** piecewise constant

$$\mathcal{Q}_F(Dh, Dv; \alpha) = \alpha \|Dh\|_{2,1} + \|Dv\|_{2,1}$$

Functionals with either free or co-localized contours

$$\underset{h,v}{\text{minimize}} \quad \sum_a \frac{\|\log \mathcal{L}_{a,.} - \log(a)h - v\|^2}{\text{Least-Squares}} + \theta \frac{\mathcal{Q}(Dh, Dv; \alpha)}{\text{Total Variation}}$$

\rightarrow fidelity to the log-linear model
 \rightarrow favors piecewise constancy



Finite differences $Dh = [D_1 h, D_2 h]$

Free: h, v are **independently** piecewise constant

$$\mathcal{Q}_F(Dh, Dv; \alpha) = \alpha \|Dh\|_{2,1} + \|Dv\|_{2,1}$$

Co-localized: h, v are **concomitantly** piecewise constant

$$\mathcal{Q}_C(Dh, Dv; \alpha) = \|[\alpha Dh, Dv]\|_{2,1}$$

Functionals minimization

$$\underset{h,v}{\text{minimize}} \quad \sum_a \frac{\|\log \mathcal{L}_{a,\cdot} - \log(a)h - v\|^2}{\text{Least-Squares}} + \theta \frac{\mathcal{Q}(Dh, Dv; \alpha)}{\text{Total Variation}}$$



Functionals minimization

$$\underset{h,v}{\text{minimize}} \quad \sum_a \frac{\|\log \mathcal{L}_{a,\cdot} - \log(a)h - v\|^2}{\text{Least-Squares}} + \theta \frac{\mathcal{Q}(Dh, Dv; \alpha)}{\text{Total Variation}}$$



- gradient descent $x^{[k+1]} = x^{[k]} - \tau \nabla f(x^{[k]})$ $x = (h, v)$

Functionals minimization

$$\underset{h,v}{\text{minimize}} \quad \sum_a \frac{\|\log \mathcal{L}_{a,.} - \log(a)h - v\|^2}{\text{Least-Squares}} + \theta \frac{\mathcal{Q}(Dh, Dv; \alpha)}{\text{Total Variation}}$$



nonsmooth



- ▶ gradient descent $x^{[k+1]} = x^{[k]} - \tau \nabla f(x^{[k]})$ $x = (h, v)$
- ▶ implicit subgradient descent: proximal point algorithm

$$x^{[k+1]} = x^{[k]} - \tau u^{[k]}, \quad u^{[k]} \in \partial f(x^{[k+1]}) \Leftrightarrow x^{[k+1]} = \text{prox}_{\tau f}(x^{[k]})$$

Functionals minimization

$$\underset{h,v}{\text{minimize}} \quad \sum_a \frac{\|\log \mathcal{L}_{a,.} - \log(a)h - v\|^2}{\text{Least-Squares}} + \theta \frac{\mathcal{Q}(Dh, Dv; \alpha)}{\text{Total Variation}}$$



nonsmooth



- ▶ gradient descent $x^{[k+1]} = x^{[k]} - \tau \nabla f(x^{[k]})$ $x = (h, v)$
- ▶ implicit subgradient descent: proximal point algorithm
 $x^{[k+1]} = x^{[k]} - \tau u^{[k]}, u^{[k]} \in \partial f(x^{[k+1]}) \Leftrightarrow x^{[k+1]} = \text{prox}_{\tau f}(x^{[k]})$
- ▶ splitting proximal algorithm
 - $u^{[k+1]} = \text{prox}_{\sigma(\theta \mathcal{Q})^*} \left(u^{[k]} + \sigma D \bar{x}^{[k]} \right)$
 - $x^{[k+1]} = \text{prox}_{\tau \|\mathcal{L} - A\cdot\|_2^2} \left(x^{[k]} - \tau D^\top u^{[k+1]} \right), \quad A : (h, v) \mapsto \{\log(a)h + v\}_a$
 - $\bar{x}^{[k+1]} = 2x^{[k+1]} - x^{[k]}$ [A. Chambolle et al., 2011, *J. Math. Imaging Vis.*]

Functionals minimization

$$\underset{h,v}{\text{minimize}} \quad \sum_a \frac{\|\log \mathcal{L}_{a,\cdot} - \log(a)h - v\|^2}{\text{Least-Squares}} + \theta \frac{\mathcal{Q}(Dh, Dv; \alpha)}{\text{Total Variation}}$$



nonsmooth



- ▶ gradient descent $x^{[k+1]} = x^{[k]} - \tau \nabla f(x^{[k]})$ $x = (h, v)$
- ▶ implicit subgradient descent: proximal point algorithm
 $x^{[k+1]} = x^{[k]} - \tau u^{[k]}, u^{[k]} \in \partial f(x^{[k+1]}) \Leftrightarrow x^{[k+1]} = \text{prox}_{\tau f}(x^{[k]})$
- ▶ splitting proximal algorithm
 - $u^{[k+1]} = \text{prox}_{\sigma(\theta \mathcal{Q})^*} \left(u^{[k]} + \sigma D \bar{x}^{[k]} \right)$
 - $x^{[k+1]} = \text{prox}_{\tau \|\mathcal{L} - A\|_2^2} \left(x^{[k]} - \tau D^\top u^{[k+1]} \right), \quad A : (h, v) \mapsto \{\log(a)h + v\}_a$
 - $\bar{x}^{[k+1]} = 2x^{[k+1]} - x^{[k]}$ [A. Chambolle et al., 2011, *J. Math. Imaging Vis.*]

Accelerated algorithm based on strong-convexity

$$\underset{h,v}{\text{minimize}} \quad \sum_a \frac{\|\log \mathcal{L}_{a,:} - \log(a)h - v\|^2}{\text{Least-Squares}} + \theta \frac{\mathcal{Q}(Dh, Dv; \alpha)}{\text{Total Variation}}$$



nonsmooth



Primal-dual algorithm [A. Chambolle et al., 2011, *J. Math. Imaging Vis.*]

$$\delta: \text{duality gap}, \delta(x^{[k]}, u^{[k]}) \xrightarrow{n \rightarrow \infty} 0$$

Accelerated algorithm based on strong-convexity

$$\underset{h,v}{\text{minimize}} \quad \sum_a \frac{\|\log \mathcal{L}_{a,:} - \log(a)h - v\|^2}{\text{Least-Squares}} + \theta \frac{\mathcal{Q}(Dh, Dv; \alpha)}{\text{Total Variation}}$$

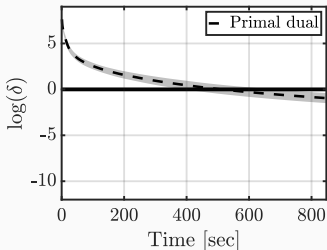


nonsmooth



Primal-dual algorithm [A. Chambolle et al., 2011, *J. Math. Imaging Vis.*]

$$\delta: \text{duality gap}, \delta(x^{[k]}, u^{[k]}) \xrightarrow[n \rightarrow \infty]{} 0$$



Convexity properties

$$\underset{h,v}{\text{minimize}} \quad \sum_a \frac{\|\log \mathcal{L}_{a,.} - \log(a)h - v\|^2}{\text{Least-Squares}} + \theta \frac{\mathcal{Q}(Dh, Dv; \alpha)}{\text{Total Variation}}$$



ρ -strongly convex



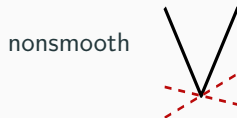
nonsmooth

Convexity properties

$$\underset{h,v}{\text{minimize}} \quad \sum_a \frac{\|\log \mathcal{L}_{a,.} - \log(a)h - v\|^2}{\text{Least-Squares}} + \theta \frac{\mathcal{Q}(Dh, Dv; \alpha)}{\text{Total Variation}}$$



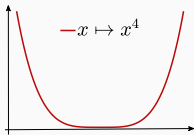
ρ -strongly convex



nonsmooth

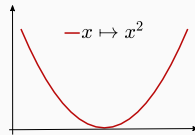
Strong-convexity

- f ρ -strongly convex iff $f - \frac{\rho}{2}\|\cdot\|^2$ convex



✓ strictly convex

✗ non strongly convex



✓ strictly convex

✓ 1-strongly convex

Convexity properties

$$\underset{h,v}{\text{minimize}} \quad \sum_a \frac{\|\log \mathcal{L}_{a,.} - \log(a)h - v\|^2}{\text{Least-Squares}} + \theta \frac{\mathcal{Q}(Dh, Dv; \alpha)}{\text{Total Variation}}$$



ρ -strongly convex

nonsmooth



Strong-convexity

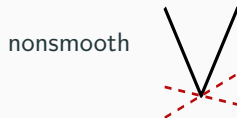
- f ρ -strongly convex iff $f - \frac{\rho}{2}\|\cdot\|^2$ convex
- $f \in \mathcal{C}^2$ with Hessian matrix $Hf \succeq 0 \implies \rho = \min \text{Sp}(Hf)$

Convexity properties

$$\underset{h,v}{\text{minimize}} \quad \sum_a \frac{\|\log \mathcal{L}_{a,.} - \log(a)h - v\|^2}{\text{Least-Squares}} + \theta \frac{\mathcal{Q}(Dh, Dv; \alpha)}{\text{Total Variation}}$$



ρ -strongly convex



nonsmooth

Strong-convexity

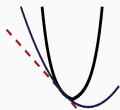
- f ρ -strongly convex iff $f - \frac{\rho}{2}\|\cdot\|^2$ convex
- $f \in \mathcal{C}^2$ with Hessian matrix $Hf \succeq 0 \implies \rho = \min \text{Sp}(Hf)$

Proposition $\sum_a \|\log \mathcal{L}_a - \log(a)h - v\|^2$ is ρ -strongly convex.

$a_{\min} = 2^1$,	a_{\max}	2^2	2^3	2^4	2^5	2^6
$\rho = \min \text{Sp}(A^\top A)$		0.29	0.72	1.20	1.69	2.20

Accelerated algorithm based on strong-convexity

$$\underset{h,v}{\text{minimize}} \quad \sum_a \frac{\|\log \mathcal{L}_{a,.} - \log(a)h - v\|^2}{\text{Least-Squares}} + \theta \frac{\mathcal{Q}(Dh, Dv; \alpha)}{\text{Total Variation}}$$



ρ -strongly convex



nonsmooth

Accelerated Primal-dual algorithm [A. Chambolle et al., 2011, *J. Math. Imaging Vis.*]

for $k = 0, 1, \dots$ $x = (h, v)$

$$u^{[k+1]} = \text{prox}_{\sigma_k(\theta\mathcal{Q})^*} \left(u^{[k]} + \sigma_k D\bar{x}^{[k]} \right)$$

$$x^{[k+1]} = \text{prox}_{\tau_k \|\mathcal{L}-A\cdot\|_2^2} \left(x^{[k]} - \tau_k D^\top u^{[k+1]} \right)$$

$$\theta_k = \sqrt{1 + 2\rho\tau_k}, \quad \tau_{n+1} = \tau_k/\theta_k, \quad \sigma_{n+1} = \theta_k \sigma_k$$

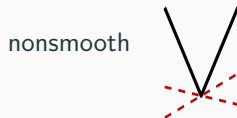
$$\bar{x}^{[k+1]} = x^{[k+1]} + \theta_k^{-1} \left(x^{[k+1]} - x^{[k]} \right)$$

Accelerated algorithm based on strong-convexity

$$\underset{h,v}{\text{minimize}} \quad \sum_a \frac{\|\log \mathcal{L}_{a,.} - \log(a)h - v\|^2}{\text{Least-Squares}} + \theta \frac{\mathcal{Q}(Dh, Dv; \alpha)}{\text{Total Variation}}$$



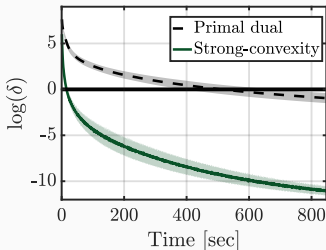
ρ -strongly convex



nonsmooth

Accelerated Primal-dual algorithm [A. Chambolle et al., 2011, *J. Math. Imaging Vis.*]

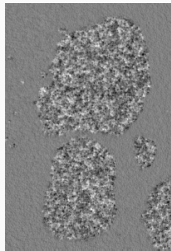
$$\delta: \text{duality gap}, \delta(x^{[k]}, u^{[k]}) \xrightarrow[n \rightarrow \infty]{} 0$$



Segmentation via iterated thresholding

$$\underset{h,v}{\text{minimize}} \sum_a \frac{\|\log \mathcal{L}_{a,.} - \log(a)h - v\|^2}{\text{Least-Squares}} + \theta \frac{\mathcal{Q}(Dh, Dv; \alpha)}{\text{Total Variation}}$$

Textured image Lin. reg. \hat{h}^{LR}

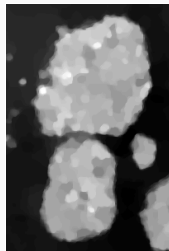
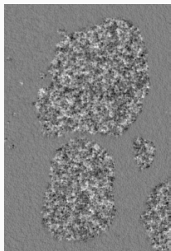


Segmentation via iterated thresholding

$$\underset{h,v}{\text{minimize}} \quad \sum_a \frac{\|\log \mathcal{L}_{a,.} - \log(a)h - v\|^2}{\text{Least-Squares}} + \theta \frac{\mathcal{Q}(Dh, Dv; \alpha)}{\text{Total Variation}}$$

Textured image Lin. reg. \hat{h}^{LR} Co-localized contours \hat{h}^{C} Threshold estimate[†] $T\hat{h}^{\text{C}}$

[B. Pascal et al., 2021, *Appl. Comput. Harmon. Anal.*]



†Thresholding strategy from: [X. Cai et al., 2013, *EMMCVPR*]

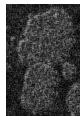
State-of-the-art methods for texture segmentation

Threshold-ROF on \hat{h}^{LR}

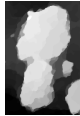
[C. Naftornita et al., 2014, *ICIP*; N. Pustelnik et
al., 2016, *IEEE Trans. Comput. Imaging*]

$$\operatorname{argmin}_h \|h - \hat{h}^{\text{LR}}\|^2 + \theta \|Dh\|_{2,1}$$

Lin. reg.



ROF



Threshold



Only based on regularity h.

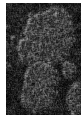
State-of-the-art methods for texture segmentation

Threshold-ROF on \hat{h}^{LR}

[C. Naftornita et al., 2014, *ICIP*; N. Pustelnik et al., 2016, *IEEE Trans. Comput. Imaging*]

$$\operatorname{argmin}_h \|h - \hat{h}^{\text{LR}}\|^2 + \theta \|Dh\|_{2,1}$$

Lin. reg.



ROF



Threshold

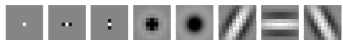


Only based on regularity h.

Factorization based segmentation[†]

[J. Yuan, 2015, *IEEE Trans. Image Process.*]

(i) local histograms



(ii) matrix factorization

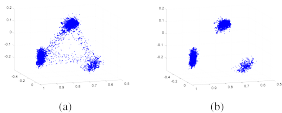


Fig. 2. Scatterplot of features in subspace. (a) Scatterplot of features projected onto the 3-d subspace. (b) Scatterplot after removing features with high edgeness.

[†]<https://sites.google.com/site/factorizationsegmentation/>

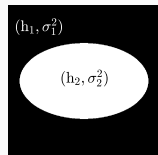
Compared segmentation performance on synthetic textures

Piecewise monofractal texture synthesis

[B. Pascal et al., 2021, *Appl. Comput. Harmon. Anal.*]

mask: $\Omega = \Omega_1 \sqcup \Omega_2$,

attributes: $(H_\ell, \sigma_\ell^2)_{\ell=1,2}$



Compared segmentation performance on synthetic textures

Piecewise monofractal texture synthesis

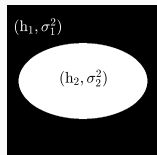
[B. Pascal et al., 2021, *Appl. Comput. Harmon. Anal.*]

mask: $\Omega = \Omega_1 \sqcup \Omega_2$,

attributes: $(H_\ell, \sigma_\ell^2)_{\ell=1,2}$

Ex. $H_1 = 0.5, \sigma_1^2 = 0.6$

$H_2 = 0.6, \sigma_2^2 = 0.7$



Compared segmentation performance on synthetic textures

Piecewise monofractal texture synthesis

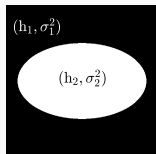
[B. Pascal et al., 2021, *Appl. Comput. Harmon. Anal.*]

mask: $\Omega = \Omega_1 \sqcup \Omega_2$,

attributes: $(H_\ell, \sigma_\ell^2)_{\ell=1,2}$

Ex. $H_1 = 0.5, \sigma_1^2 = 0.6$

$H_2 = 0.6, \sigma_2^2 = 0.7$



Averaged segmentation performances over 5 realizations

Yuan



T-ROF



free



co-localized
contours



$71.1 \pm 1.3\%$

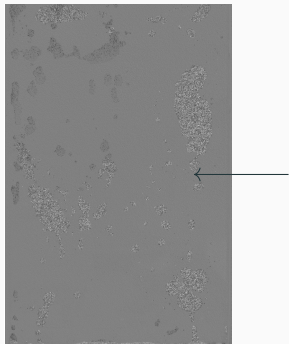
$78.5 \pm 1.1\%$

$90.2 \pm 1.9\%$

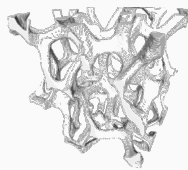
$91.1 \pm 1.5\%$

Multiphase flow through porous media

Laboratoire de Physique, ENS Lyon, V. Vidal, T. Busser, (M. Serres, IFPEN)

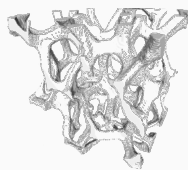
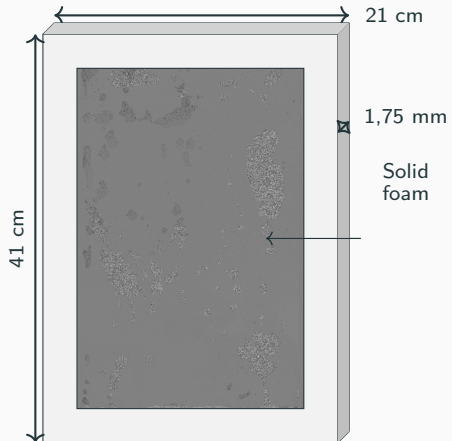


Solid
foam



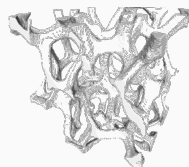
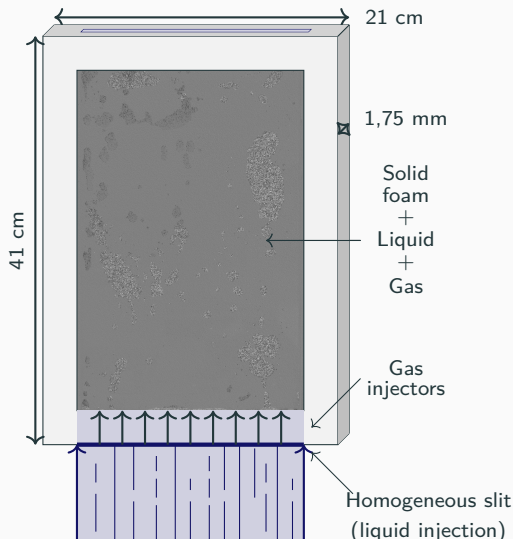
Multiphase flow through porous media

Laboratoire de Physique, ENS Lyon, V. Vidal, T. Busser, (M. Serres, IFPEN)



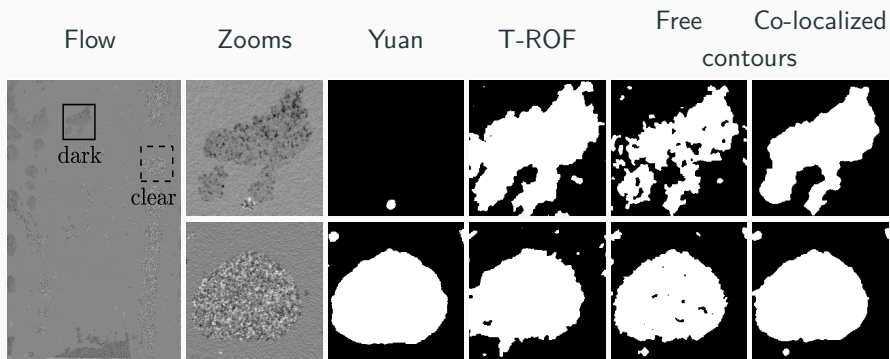
Multiphase flow through porous media

Laboratoire de Physique, ENS Lyon, V. Vidal, T. Busser, (M. Serres, IFPEN)

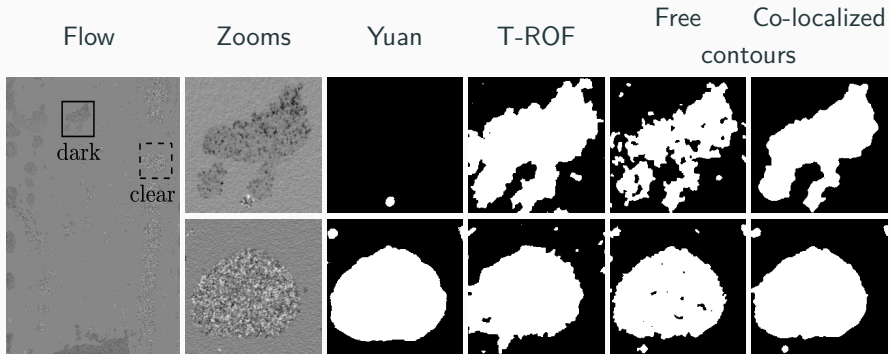


→ 1600×1100 pixels
→ video: ~ 1000 images
→ phase diagram: ~ 10 flow
rates

Low activity: $Q_G = 300\text{mL/min}$ - $Q_L = 300\text{mL/min}$



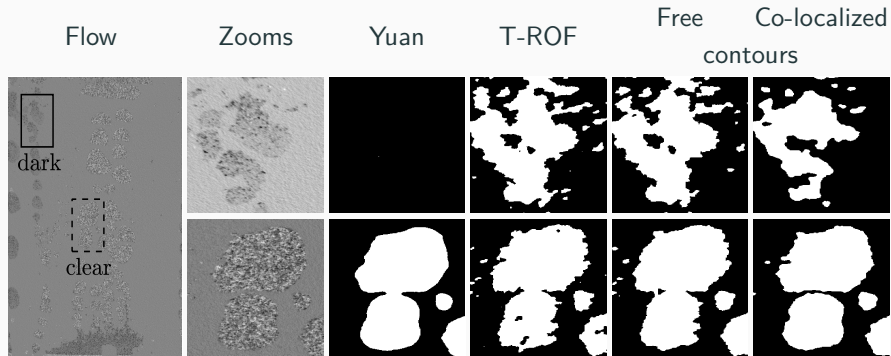
Low activity: $Q_G = 300\text{mL/min}$ - $Q_L = 300\text{mL/min}$



$$\text{Liquid: } H_L = 0.4 \quad \sigma_{\text{dark}}^2 = 10^{-2}$$

$$\text{Gas: } H_G = 0.9 \quad \left| \begin{array}{ll} \sigma_{\text{dark}}^2 = 10^{-2} & \text{(dark bubbles)} \\ \sigma_{\text{clear}}^2 = 10^{-1} & \text{(clear bubbles)} \end{array} \right.$$

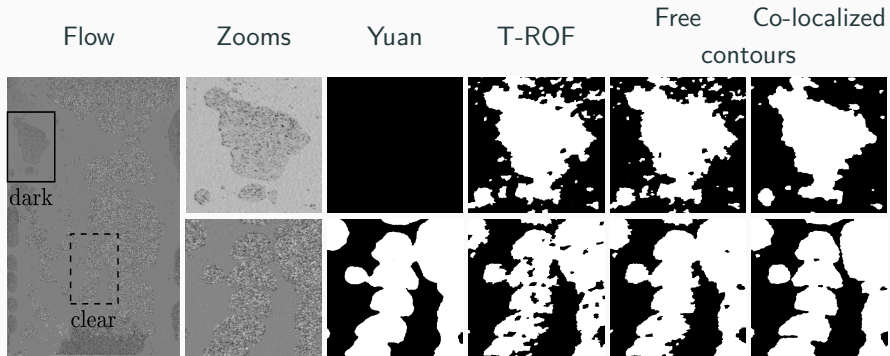
Transition: $Q_G = 400 \text{mL/min}$ - $Q_L = 700 \text{mL/min}$



$$\text{Liquid: } H_L = 0.4 \quad \sigma_{\text{dark}}^2 = 10^{-2}$$

$$\text{Gas: } H_G = 0.9 \quad \left| \begin{array}{ll} \sigma_{\text{dark}}^2 = 10^{-2} & \text{(dark bubbles)} \\ \sigma_{\text{clear}}^2 = 10^{-1} & \text{(clear bubbles)} \end{array} \right.$$

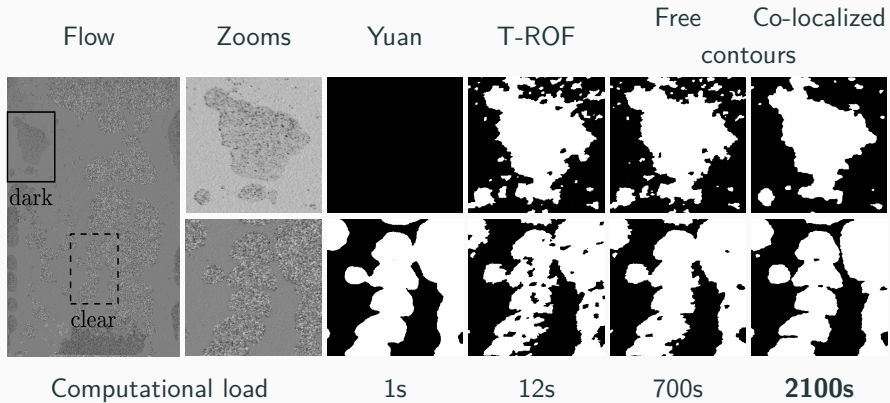
High activity: $Q_G = 1200 \text{mL/min}$ - $Q_L = 300 \text{mL/min}$



$$\text{Liquid: } H_L = 0.4 \quad \sigma_{\text{dark}}^2 = 10^{-2}$$

$$\text{Gas: } H_G = 0.9 \quad \left| \begin{array}{ll} \sigma_{\text{dark}}^2 = 10^{-2} & \text{(dark bubbles)} \\ \sigma_{\text{clear}}^2 = 10^{-1} & \text{(clear bubbles)} \end{array} \right.$$

High activity: $Q_G = 1200 \text{mL/min}$ - $Q_L = 300 \text{mL/min}$



Liquid: $H_L = 0.4$ $\sigma_{\text{dark}}^2 = 10^{-2}$

Gas: $H_G = 0.9$ $\left| \begin{array}{ll} \sigma_{\text{dark}}^2 = 10^{-2} & \text{(dark bubbles)} \\ \sigma_{\text{clear}}^2 = 10^{-1} & \text{(clear bubbles)} \end{array} \right.$

Regularization parameters selection

$$(\hat{h}, \hat{v}) (\mathcal{L}; \Theta) = \operatorname{argmin}_{h, v} \sum_a \|\log \mathcal{L}_{a,.} - \log(a)h - v\|^2 + \theta_1 \mathcal{Q}(Dh, Dv; \theta_2)$$

Regularization parameters selection

$$(\hat{h}, \hat{v}) (\mathcal{L}; \Theta) = \operatorname{argmin}_{h, v} \sum_a \|\log \mathcal{L}_{a,.} - \log(a)h - v\|^2 + \theta_1 \mathcal{Q}(Dh, Dv; \theta_2)$$

Lin. reg. \hat{h}^{LR}

$$(\theta_1, \theta_2) = (0, 0)$$



Regularization parameters selection

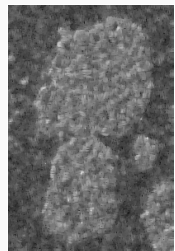
$$(\hat{h}, \hat{v}) (\mathcal{L}; \Theta) = \operatorname{argmin}_{h, v} \sum_a \|\log \mathcal{L}_{a,.} - \log(a)h - v\|^2 + \theta_1 \mathcal{Q}(Dh, Dv; \theta_2)$$

Lin. reg. \hat{h}^{LR}

$$(\theta_1, \theta_2) = (0, 0) \quad (\theta_1, \theta_2) = (0.5, 0.5)$$



Co-localized contours estimate \hat{h}^C



too small

Regularization parameters selection

$$\left(\hat{h}, \hat{v}\right)(\mathcal{L}; \Theta) = \operatorname{argmin}_{h, v} \sum_a \|\log \mathcal{L}_{a,.} - \log(a)h - v\|^2 + \theta_1 \mathcal{Q}(Dh, Dv; \theta_2)$$

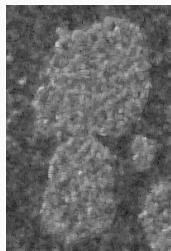
Lin. reg. \hat{h}^{LR}

$$(\theta_1, \theta_2) = (0, 0)$$



Co-localized contours estimate \hat{h}^C

$$(\theta_1, \theta_2) = (0.5, 0.5)$$



$$(\theta_1, \theta_2) = (500, 500)$$



too small

too large

Regularization parameters selection

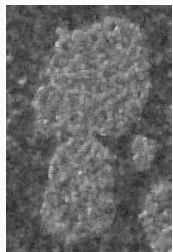
$$(\hat{h}, \hat{v}) (\mathcal{L}; \Theta) = \operatorname{argmin}_{h, v} \sum_a \|\log \mathcal{L}_{a,.} - \log(a)h - v\|^2 + \theta_1 \mathcal{Q}(Dh, Dv; \theta_2)$$

Lin. reg. \hat{h}^{LR}

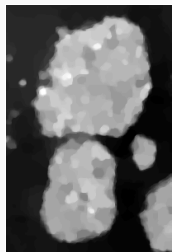


Co-localized contours estimate \hat{h}^C

$$(\theta_1, \theta_2) = (0, 0) \quad (\theta_1, \theta_2) = (0.5, 0.5) \quad (\theta_1^\dagger, \theta_2^\dagger) = (11.5, 0.8) \quad (\theta_1, \theta_2) = (500, 500)$$



too small



optimal



too large

What *optimal* means? How to determine $\Theta^\dagger = (\theta_1^\dagger, \theta_2^\dagger)$?

Parameter tuning (Grid search)

$$\left(\hat{\mathbf{h}}, \hat{\mathbf{v}}\right) (\mathcal{L}; \Theta) = \operatorname{argmin}_{\mathbf{h}, \mathbf{v}} \sum_a \|\log \mathcal{L}_{a,.} - \log(a)\mathbf{h} - \mathbf{v}\|^2 + \theta_1 \mathcal{Q}(\mathbf{D}\mathbf{h}, \mathbf{D}\mathbf{v}; \theta_2)$$

\mathbf{h} : *discriminant*, \mathbf{v} : *auxiliary*

Parameter tuning (Grid search)

$$\left(\hat{\mathbf{h}}, \hat{\mathbf{v}}\right)(\mathcal{L}; \Theta) = \underset{\mathbf{h}, \mathbf{v}}{\operatorname{argmin}} \sum_a \|\log \mathcal{L}_{a,.} - \log(a)\mathbf{h} - \mathbf{v}\|^2 + \theta_1 \mathcal{Q}(\mathbf{D}\mathbf{h}, \mathbf{D}\mathbf{v}; \theta_2)$$

\mathbf{h} : *discriminant*, \mathbf{v} : *auxiliary*

$\bar{\mathbf{h}}$: *true regularity*

$$\mathcal{R}(\Theta) = \left\| \hat{\mathbf{h}}(\mathcal{L}; \Theta) - \bar{\mathbf{h}} \right\|^2$$

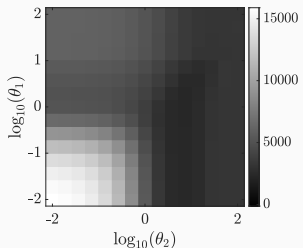
Parameter tuning (Grid search)

$$(\hat{\mathbf{h}}, \hat{\mathbf{v}}) (\mathcal{L}; \Theta) = \underset{\mathbf{h}, \mathbf{v}}{\operatorname{argmin}} \sum_a \|\log \mathcal{L}_{a,.} - \log(a) \mathbf{h} - \mathbf{v}\|^2 + \theta_1 \mathcal{Q}(\mathbf{D}\mathbf{h}, \mathbf{D}\mathbf{v}; \theta_2)$$

\mathbf{h} : *discriminant*, \mathbf{v} : *auxiliary*

$\bar{\mathbf{h}}$: *true regularity*

$$\mathcal{R}(\Theta) = \left\| \hat{\mathbf{h}}(\mathcal{L}; \Theta) - \bar{\mathbf{h}} \right\|^2$$



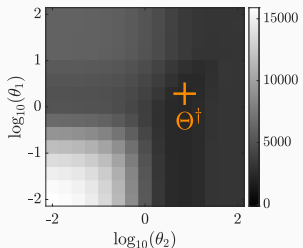
Parameter tuning (Grid search)

$$\left(\hat{\mathbf{h}}, \hat{\mathbf{v}}\right) (\mathcal{L}; \Theta) = \operatorname{argmin}_{\mathbf{h}, \mathbf{v}} \sum_a \|\log \mathcal{L}_{a,.} - \log(a) \mathbf{h} - \mathbf{v}\|^2 + \theta_1 \mathcal{Q}(\mathbf{D}\mathbf{h}, \mathbf{D}\mathbf{v}; \theta_2)$$

\mathbf{h} : *discriminant*, \mathbf{v} : *auxiliary*

$\bar{\mathbf{h}}$: *true regularity*

$$\mathcal{R}(\Theta) = \left\| \hat{\mathbf{h}}(\mathcal{L}; \Theta) - \bar{\mathbf{h}} \right\|^2$$



Parameter tuning (Grid search)

$$(\widehat{\mathbf{h}}, \widehat{\mathbf{v}}) (\mathcal{L}; \Theta) = \operatorname{argmin}_{\mathbf{h}, \mathbf{v}} \sum_a \|\log \mathcal{L}_{a,.} - \log(a) \mathbf{h} - \mathbf{v}\|^2 + \theta_1 \mathcal{Q}(\mathbf{D}\mathbf{h}, \mathbf{D}\mathbf{v}; \theta_2)$$

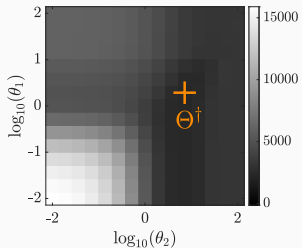
\mathbf{h} : *discriminant*, \mathbf{v} : *auxiliary*

$\bar{\mathbf{h}}$: *true regularity*

$\bar{\mathbf{h}}$: *unknown!*

$$\mathcal{R}(\Theta) = \left\| \widehat{\mathbf{h}}(\mathcal{L}; \Theta) - \bar{\mathbf{h}} \right\|^2$$

?



Parameter tuning (Grid search)

$$(\widehat{\mathbf{h}}, \widehat{\mathbf{v}}) (\mathcal{L}; \Theta) = \operatorname{argmin}_{\mathbf{h}, \mathbf{v}} \sum_a \|\log \mathcal{L}_{a,.} - \log(a) \mathbf{h} - \mathbf{v}\|^2 + \theta_1 \mathcal{Q}(\mathbf{D}\mathbf{h}, \mathbf{D}\mathbf{v}; \theta_2)$$

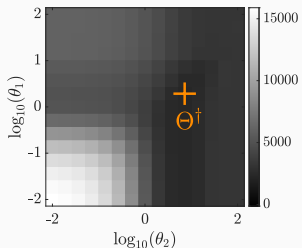
\mathbf{h} : *discriminant*, \mathbf{v} : *auxiliary*

$\bar{\mathbf{h}}$: *true regularity*

$$\mathcal{R}(\Theta) = \left\| \widehat{\mathbf{h}}(\mathcal{L}; \Theta) - \bar{\mathbf{h}} \right\|^2$$

$\bar{\mathbf{h}}$: *unknown!*

?



*Stein Unbiased Risk
Estimate
(SURE)*

Stein Unbiased Risk Estimate (Principle)

Observations $z = \bar{x} + n \in \mathbb{R}^P$, \bar{x} : truth and $n \sim \mathcal{N}(0, \kappa^2 I_P)$

Stein Unbiased Risk Estimate (Principle)

Observations $z = \bar{x} + n \in \mathbb{R}^P$, \bar{x} : truth and $n \sim \mathcal{N}(0, \kappa^2 I_P)$

Parametric estimator $(z; \theta) \mapsto \hat{x}(z; \theta)$

Ex. $\hat{x}(z; \theta) = \begin{cases} (I + \theta D^\top D)^{-1} z & (\text{linear}) \\ \underset{x}{\operatorname{argmin}} \|z - x\|^2 + \theta \mathcal{Q}(Dx) & (\text{nonlinear}) \end{cases}$

Stein Unbiased Risk Estimate (Principle)

Observations $z = \bar{x} + n \in \mathbb{R}^P$, \bar{x} : truth and $n \sim \mathcal{N}(0, \kappa^2 I_P)$

Parametric estimator $(z; \theta) \mapsto \hat{x}(z; \theta)$

Ex. $\hat{x}(z; \theta) = \begin{cases} (I + \theta D^\top D)^{-1} z & (\text{linear}) \\ \underset{x}{\operatorname{argmin}} \|z - x\|^2 + \theta \mathcal{Q}(Dx) & (\text{nonlinear}) \end{cases}$

Quadratic error $R(\theta) \triangleq \mathbb{E}_n \|\hat{x}(z; \theta) - \bar{x}\|^2 \stackrel{?}{=} \mathbb{E}_n \hat{R}(z; \theta)$ \bar{x} unknown

Stein Unbiased Risk Estimate (Principle)

Observations $z = \bar{x} + n \in \mathbb{R}^P$, \bar{x} : truth and $n \sim \mathcal{N}(0, \kappa^2 I_P)$

Parametric estimator $(z; \theta) \mapsto \hat{x}(z; \theta)$

Ex. $\hat{x}(z; \theta) = \begin{cases} (I + \theta D^\top D)^{-1} z & \text{(linear)} \\ \underset{x}{\operatorname{argmin}} \|z - x\|^2 + \theta \mathcal{Q}(Dx) & \text{(nonlinear)} \end{cases}$

Quadratic error $R(\theta) \triangleq \mathbb{E}_n \|\hat{x}(z; \theta) - \bar{x}\|^2 \stackrel{?}{=} \mathbb{E}_n \widehat{R}(z; \theta)$ \bar{x} unknown

Theorem [C. M. Stein, 1981, *Annals Stat.*]

Let $(z; \theta) \mapsto \hat{x}(z; \theta)$ an estimator of \bar{x}

- weakly differentiable w.r.t. z ,
- such that $n \mapsto \langle \hat{x}(\bar{x} + n; \theta), n \rangle$ is integrable w.r.t. $\mathcal{N}(0, \kappa^2 I_P)$.

$$\begin{aligned} \widehat{R}(z; \theta) &\triangleq \|\hat{x}(z; \theta) - z\|^2 + 2\kappa^2 \operatorname{tr} (\partial_z \hat{x}(z; \theta)) - \kappa^2 P \\ &\implies R(\theta) = \mathbb{E}_n [\widehat{R}(z; \theta)]. \end{aligned}$$

Generalized Stein Unbiased Risk Estimate

Observations $\mathbf{z} = \mathbf{A}\bar{\mathbf{x}} + \mathbf{n} \in \mathbb{R}^P$, $\bar{\mathbf{x}} \in \mathbb{R}^N$, $\mathbf{A} : \mathbb{R}^{P \times N}$ and $\mathbf{n} \sim \mathcal{N}(0, \mathcal{S})$

E.g. the estimators $\hat{h}(\mathcal{L}; \Theta)$ with free or co-localized contours

$$\log \mathcal{L} = \mathbf{A}(\bar{h}, \bar{v}) + \mathbf{n} \quad n \sim \mathcal{N}(0, \mathcal{S}) \quad \mathcal{R} = \|\hat{h} - \bar{h}\|^2$$

$$\mathbf{A} : (h, v) \mapsto \{\log(a)h + v\}_a \quad \begin{array}{|c|c|c|c|c|c|c|c|c|} \hline & \cdot \\ \hline \cdot & \cdot \\ \hline \end{array} \quad \Pi : (h, v) \mapsto (h, 0)$$

Projected estimation error $R_\Pi(\Theta) \triangleq \mathbb{E}_n \|\Pi \hat{\mathbf{x}}(\mathbf{z}; \Theta) - \Pi \bar{\mathbf{x}}\|^2$

Generalized Stein Unbiased Risk Estimate

Observations $z = \mathbf{A}\bar{x} + n \in \mathbb{R}^P$, $\bar{x} \in \mathbb{R}^N$, $\mathbf{A} : \mathbb{R}^{P \times N}$ and $n \sim \mathcal{N}(0, \mathcal{S})$

E.g. the estimators $\hat{h}(\mathcal{L}; \Theta)$ with free or co-localized contours

$$\log \mathcal{L} = \mathbf{A}(\bar{h}, \bar{v}) + n \quad n \sim \mathcal{N}(0, \mathcal{S}) \quad \mathcal{R} = \|\hat{h} - \bar{h}\|^2$$

$$\mathbf{A} : (h, v) \mapsto \{\log(a)h + v\}_a \quad \begin{array}{|c|c|c|c|c|c|c|c|c|} \hline & \bullet \\ \hline \bullet & \bullet \\ \hline \end{array} \quad \text{OR} : (h, v) \mapsto (h, 0)$$

Projected estimation error $R_\Pi(\Theta) \triangleq \mathbb{E}_n \|\Pi \hat{x}(z; \Theta) - \Pi \bar{x}\|^2$

Theorem (B. Pascal et al., 2020, *J. Math. Imaging Vis.*)

Let $(z; \Theta) \mapsto \hat{x}(z; \Theta)$ an estimator of \bar{x}

- weakly differentiable w.r.t. z ,
- such that $n \mapsto \langle \Pi \hat{x}(\bar{x} + n; \Theta), \Phi n \rangle$ is integrable w.r.t. $\mathcal{N}(0, \mathcal{S})$.

$$\begin{aligned} \hat{R}(\Theta) &\triangleq \|\Phi(\mathbf{A}\hat{x}(z; \Theta) - z)\|^2 + 2\text{tr}(\mathcal{S}\Phi^\top \Pi \partial_z \hat{x}(z; \Theta)) - \text{tr}(\Phi \mathcal{S} \Phi^\top) \\ &\implies R_\Pi(\Theta) = \mathbb{E}_n [\hat{R}(\Theta)]. \end{aligned}$$

Computation of the degrees of freedom

Degrees of freedom $dof \triangleq \text{tr} (\mathcal{S}\Phi^\top \Pi \partial_z \hat{x}(z; \Theta))$

Computation of the degrees of freedom

Degrees of freedom $\text{dof} \triangleq \text{tr} (\mathcal{S}\Phi^\top \Pi \partial_z \hat{x}(z; \Theta))$

- Monte Carlo strategy (MC) Large size matrix $M \in \mathbb{R}^{P \times P}$

$$\text{tr}(M) = \mathbb{E}_\varepsilon \langle M\varepsilon, \varepsilon \rangle, \quad \varepsilon \sim \mathcal{N}(0, I_P)$$

Computation of the degrees of freedom

Degrees of freedom $\text{dof} \triangleq \text{tr} (\mathcal{S}\Phi^\top \Pi \partial_z \hat{x}(z; \Theta))$

- **Monte Carlo strategy** (MC) **Large size matrix** $M \in \mathbb{R}^{P \times P}$

$$\text{tr}(M) = \mathbb{E}_\varepsilon \langle M\varepsilon, \varepsilon \rangle, \quad \varepsilon \sim \mathcal{N}(0, I_P)$$

- **Finite Differences** (FD) **Inaccessible Jacobian matrix**

$$\partial_z \hat{x} [\varepsilon] \underset{\nu \rightarrow 0}{\simeq} \frac{1}{\nu} (\hat{x}(z + \nu\varepsilon; \Theta) - \hat{x}(z; \Theta))$$

Computation of the degrees of freedom

Degrees of freedom $\text{dof} \triangleq \text{tr} (\mathcal{S} \Phi^\top \Pi \partial_z \hat{x}(z; \Theta))$

- **Monte Carlo strategy** (MC) **Large size matrix** $M \in \mathbb{R}^{P \times P}$

$$\text{tr}(M) = \mathbb{E}_\varepsilon \langle M \varepsilon, \varepsilon \rangle, \quad \varepsilon \sim \mathcal{N}(0, I_P)$$

- **Finite Differences** (FD) **Inaccessible Jacobian matrix**

$$\partial_z \hat{x}[\varepsilon] \underset{\nu \rightarrow 0}{\simeq} \frac{1}{\nu} (\hat{x}(z + \nu \varepsilon; \Theta) - \hat{x}(z; \Theta))$$

Proposition (B. Pascal et al., 2020, *J. Math. Imaging Vis.*)

Let $(z; \Theta) \mapsto \hat{x}(z; \Theta)$ an estimator of \bar{x}

- uniformly Lipschitz continuous w.r.t. z ,
- such that $\forall \Theta \in \mathbb{R}^T, \hat{x}(0_P; \Theta) = 0_N$. Then

$$\mathbb{E}_n [\text{dof}] = \lim_{\nu \rightarrow 0} \mathbb{E}_{n, \varepsilon} \left[\frac{1}{\nu} \langle \mathcal{S} \Phi^\top \Pi (\hat{x}(z + \nu \varepsilon; \Theta) - \hat{x}(z; \Theta)), \varepsilon \rangle \right]$$

Estimation of the covariance structure of leader coefficients

Log-Gaussianity: $\log \mathcal{L} = A(\bar{h}, \bar{v}) + n$ with $n \sim \mathcal{N}(0, S)$

\implies Necessary to provide some estimate \hat{S} to compute dof and then \hat{R}

Estimation of the covariance structure of leader coefficients

Log-Gaussianity: $\log \mathcal{L} = A(\bar{h}, \bar{v}) + n$ with $n \sim \mathcal{N}(0, S)$

\Rightarrow Necessary to provide some estimate \hat{S} to compute dof and then \hat{R}

Covariance structure Noise $\zeta_{j,\underline{n}}$ on $\log \mathcal{L}_{j,\underline{n}}$ at scale 2^j and pixel $\underline{n} = (n_1, n_2)$

$$\mathcal{S}_{j,\underline{n}}^{j',\underline{n}'} \triangleq \mathbb{E} \zeta_{j,\underline{n}} \zeta_{j',\underline{n}'} = C_j^{j'} \Xi_j^{j'} (\underline{n} - \underline{n}'), \quad \text{where } C_j^{j'} \triangleq \mathbb{E} \zeta_{j,\underline{n}} \zeta_{j',\underline{n}}$$

- $C_j^{j'}$ independent of \underline{n} : inter-scale covariance
- $\Xi_j^{j'}$: stationary spatial correlations, with correlation length $\max(2^j, 2^{j'})$

Estimation of the covariance structure of leader coefficients

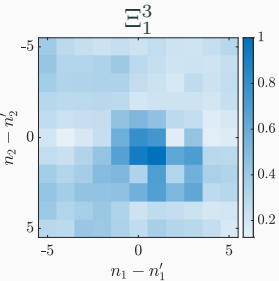
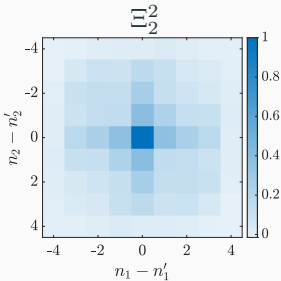
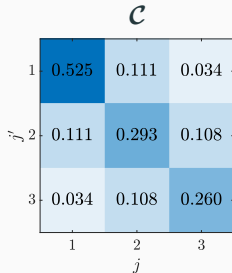
Log-Gaussianity: $\log \mathcal{L} = A(\bar{h}, \bar{v}) + n$ with $n \sim \mathcal{N}(0, \mathcal{S})$

\Rightarrow Necessary to provide some estimate \hat{S} to compute dof and then \hat{R}

Covariance structure Noise $\zeta_{j,\underline{n}}$ on $\log \mathcal{L}_{j,\underline{n}}$ at scale 2^j and pixel $\underline{n} = (n_1, n_2)$

$$\mathcal{S}_{j,\underline{n}}^{j',\underline{n}'} \triangleq \mathbb{E} \zeta_{j,\underline{n}} \zeta_{j',\underline{n}'} = \mathcal{C}_j^{j'} \Xi_j^{j'} (\underline{n} - \underline{n}'), \quad \text{where } \mathcal{C}_j^{j'} \triangleq \mathbb{E} \zeta_{j,\underline{n}} \zeta_{j',\underline{n}}$$

- $\mathcal{C}_j^{j'}$ independent of \underline{n} : inter-scale covariance
- $\Xi_j^{j'}$: stationary spatial correlations, with correlation length $\max(2^j, 2^{j'})$



Parameter tuning (Grid search)

$$\left(\hat{h}, \hat{v}\right) (\mathcal{L}; \Theta) = \operatorname{argmin}_{h, v} \sum_a \|\log \mathcal{L}_{a,.} - \log(a)h - v\|^2 + \theta_1 \mathcal{Q}(Dh, Dv; \theta_2)$$

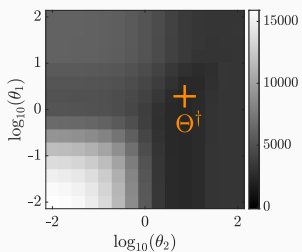
h: discriminant, v: auxiliary

\bar{h} : true regularity

\bar{h} : unknown!

$$\mathcal{R}(\Theta) = \left\| \hat{h}(\mathcal{L}; \Theta) - \bar{h} \right\|^2$$

$$\widehat{R}_{\nu, \varepsilon}(\mathcal{L}; \Theta | \mathcal{S})$$



Parameter tuning (Grid search)

$$\left(\hat{h}, \hat{v} \right) (\mathcal{L}; \Theta) = \underset{h, v}{\operatorname{argmin}} \sum_a \| \log \mathcal{L}_{a,.} - \log(a) h - v \|^2 + \theta_1 \mathcal{Q}(Dh, Dv; \theta_2)$$

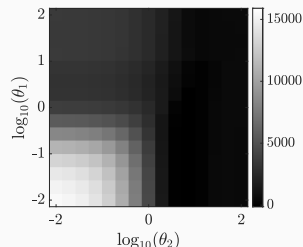
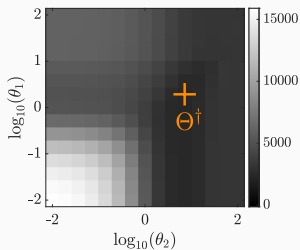
h: discriminant, v: auxiliary

\bar{h} : true regularity

$$\mathcal{R}(\Theta) = \left\| \hat{h}(\mathcal{L}; \Theta) - \bar{h} \right\|^2$$

\bar{h} : unknown!

$$\widehat{R}_{\nu, \varepsilon}(\mathcal{L}; \Theta | \mathcal{S})$$



Parameter tuning (Grid search)

$$\left(\hat{h}, \hat{v} \right) (\mathcal{L}; \Theta) = \underset{h, v}{\operatorname{argmin}} \sum_a \| \log \mathcal{L}_{a,.} - \log(a) h - v \|^2 + \theta_1 \mathcal{Q}(Dh, Dv; \theta_2)$$

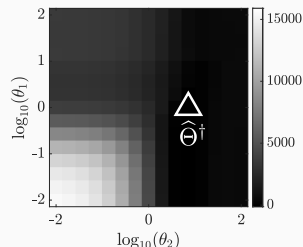
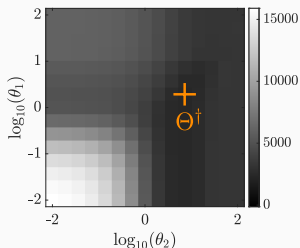
h: discriminant, v: auxiliary

\bar{h} : true regularity

$$\mathcal{R}(\Theta) = \left\| \hat{h}(\mathcal{L}; \Theta) - \bar{h} \right\|^2$$

\bar{h} : unknown!

$$\widehat{R}_{\nu, \varepsilon}(\mathcal{L}; \Theta | \mathcal{S})$$



Parameter tuning (Grid search)

$$\left(\hat{h}, \hat{v} \right) (\mathcal{L}; \Theta) = \underset{h, v}{\operatorname{argmin}} \sum_a \| \log \mathcal{L}_{a,.} - \log(a) h - v \|^2 + \theta_1 \mathcal{Q}(Dh, Dv; \theta_2)$$

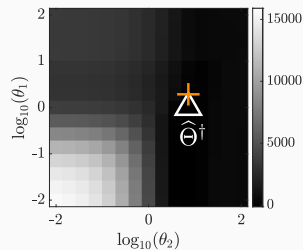
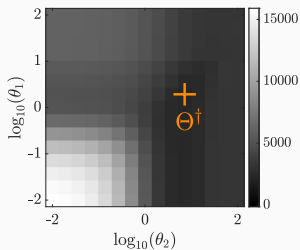
h: discriminant, v: auxiliary

\bar{h} : true regularity

$$\mathcal{R}(\Theta) = \left\| \hat{h}(\mathcal{L}; \Theta) - \bar{h} \right\|^2$$

\bar{h} : unknown!

$$\widehat{R}_{\nu, \varepsilon}(\mathcal{L}; \Theta | \mathcal{S})$$



Parameter tuning (Automatic selection)

$$\left(\hat{h}, \hat{v} \right) (\mathcal{L}; \Theta) = \underset{h, v}{\operatorname{argmin}} \sum_a \| \log \mathcal{L}_{a,.} - \log(a) h - v \|^2 + \theta_1 \mathcal{Q}(Dh, Dv; \theta_2)$$

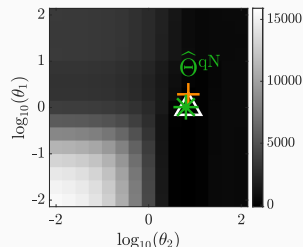
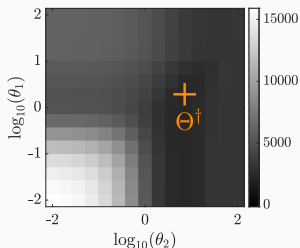
h: discriminant, v: auxiliary

\bar{h} : true regularity

$$\mathcal{R}(\Theta) = \left\| \hat{h}(\mathcal{L}; \Theta) - \bar{h} \right\|^2$$

\bar{h} : unknown!

$$\widehat{R}_{\nu, \varepsilon}(\mathcal{L}; \Theta | \mathcal{S})$$



Parameter tuning (Automatic selection)

$$\left(\hat{h}, \hat{v} \right) (\mathcal{L}; \Theta) = \underset{h, v}{\operatorname{argmin}} \sum_a \| \log \mathcal{L}_{a,.} - \log(a) h - v \|^2 + \theta_1 \mathcal{Q}(Dh, Dv; \theta_2)$$

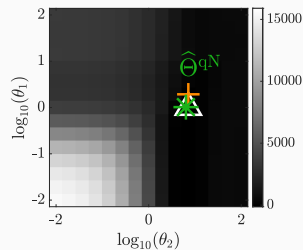
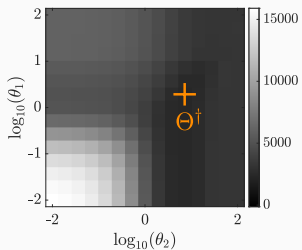
h: discriminant, v: auxiliary

\bar{h} : true regularity

$$\mathcal{R}(\Theta) = \left\| \hat{h}(\mathcal{L}; \Theta) - \bar{h} \right\|^2$$

\bar{h} : unknown!

$$\widehat{R}_{\nu, \varepsilon}(\mathcal{L}; \Theta | \mathcal{S})$$



Automated selection of regularization parameters

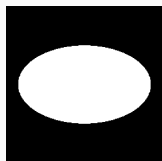
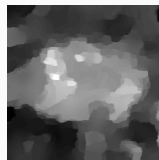
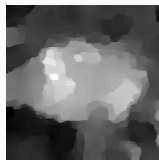
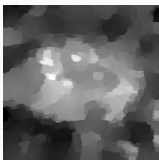
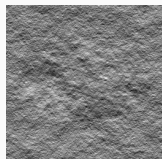
$$(\hat{h}, \hat{v}) (\mathcal{L}; \Theta) = \operatorname{argmin}_{h, v} \sum_a \|\log \mathcal{L}_{a,.} - \log(a)h - v\|^2 + \theta_1 \mathcal{Q}(Dh, Dv; \theta_2)$$

Example

$\hat{h}^F(\mathcal{L}; \Theta^\dagger)$
(grid)

$\hat{h}^F(\mathcal{L}; \hat{\Theta}^\dagger)$
(grid)

$\hat{h}^F(\mathcal{L}; \hat{\Theta}^{qN})$
(quasi-Newton)



225 calls of the estimator over the grid v.s. 40 for quasi-Newton

Isotropic texture segmentation: take home messages

- ▶ **Fractal texture model based on local *regularity* and *variance***
 - appropriate for real-world texture characterization
 - complementary attributes able to finely discriminate

Isotropic texture segmentation: take home messages

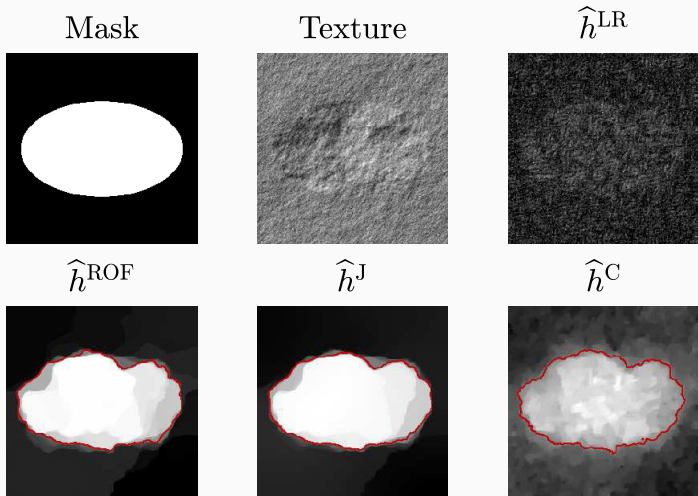
- ▶ **Fractal texture model based on local *regularity* and *variance***
 - appropriate for real-world texture characterization
 - complementary attributes able to finely discriminate

- ▶ **Simultaneous estimation and regularization**
 - significant decrease of the estimation error
 - accurate and regular *co-localized* contours

Isotropic texture segmentation: take home messages

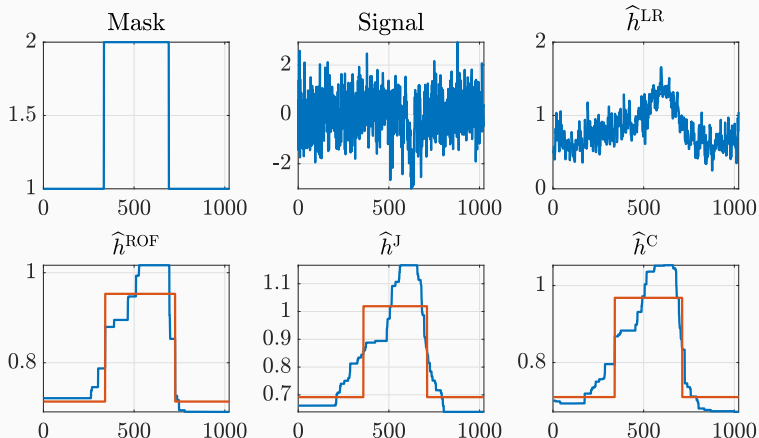
- ▶ **Fractal texture model based on local *regularity* and *variance***
 - appropriate for real-world texture characterization
 - complementary attributes able to finely discriminate
- ▶ **Simultaneous estimation and regularization**
 - significant decrease of the estimation error
 - accurate and regular *co-localized* contours
- ▶ **Fast algorithms for automated tuning of hyperparameters**
 - possibility to manage huge amount of data
 - amenable to process data corrupted by *correlated* noise
 - ensured objectivity and reproducibility

GSUGAR: Matlab toolbox for texture segmentation



github.com/bpascal-fr/gsugar: demo_gsugar_2D

GSUGAR: Changepoint detection in monofractal signals



github.com/bpascal-fr/gsugar: demo_gsugar_1D

Anisotropic textures analysis

Anisotropic fractal textures in real data

Breast cancer:

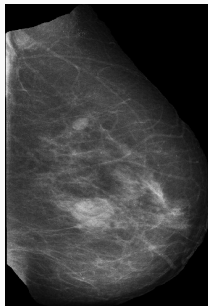
- most common cancer amongst women with ~ 1 over 8 diagnosed
- early detection is critical for the patient's survival

Anisotropic fractal textures in real data

Breast cancer:

- most common cancer amongst women with ~ 1 over 8 diagnosed
- early detection is critical for the patient's survival

X-ray imaging: most used imaging technique yielding a so-called *mammogram*

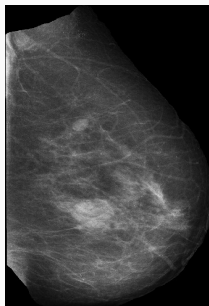


Anisotropic fractal textures in real data

Breast cancer:

- most common cancer amongst women with ~ 1 over 8 diagnosed
- early detection is critical for the patient's survival

X-ray imaging: most used imaging technique yielding a so-called *mammogram*



Assessment by a radiologist:

- fatty tissues: translucent to X-rays (black)
- epithelial & stromal tissues: absorb X-rays (white)
- tumorous tissues: **also absorb X-rays** (white)

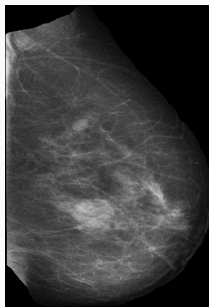
⇒ errors of both I and II types in anomaly detection

Anisotropic fractal textures in real data

Breast cancer:

- most common cancer amongst women with ~ 1 over 8 diagnosed
- early detection is critical for the patient's survival

X-ray imaging: most used imaging technique yielding a so-called *mammogram*



Assessment by a radiologist:

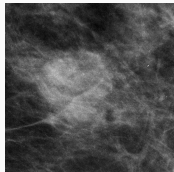
- fatty tissues: translucent to X-rays (black)
- epithelial & stromal tissues: absorb X-rays (white)
- tumorous tissues: **also absorb X-rays** (white)

⇒ errors of both I and II types in anomaly detection

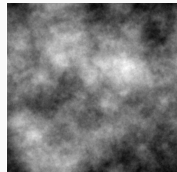
Computer-Aided Detection: used in 92% of screening mammograms in U.S.

Anisotropic fractal textures in real data

Self-similar textures:



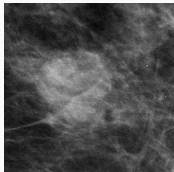
Mammogram



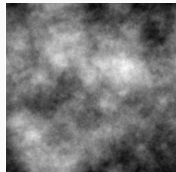
fractional Brownian field

Anisotropic fractal textures in real data

Self-similar textures:



Mammogram



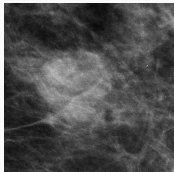
fractional Brownian field

Isotropic fractal analysis, e.g., fractal dimension of a rough surface, for

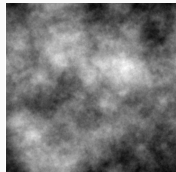
- classification of mammogram density [Caldwell et al., 1990, *Phys. Med. Biol.*]
- lesion detection in mammograms [Burgess et al., 2001, *Med. Biol.*]
- assessment of breast cancer risk [Heine et al., 2002, *Acad. Radiol.*]

Anisotropic fractal textures in real data

Self-similar textures:



Mammogram



fractional Brownian field

Isotropic fractal analysis, e.g., fractal dimension of a rough surface, for

- classification of mammogram density [Caldwell et al., 1990, *Phys. Med. Biol.*]
- lesion detection in mammograms [Burgess et al., 2001, *Med. Biol.*]
- assessment of breast cancer risk [Heine et al., 2002, *Acad. Radiol.*]

Looking for anisotropy in mammograms textures

[F. J. Richard et al., 2010, *J. Math. Imaging Vis.*; F. J. Richard, 2016, *Spat. Stat.*]

Anisotropic Self-Similar Fields

Definition: Let $f \in L^1(\min(1, |\underline{\xi}|^2)d\xi)$ a **spectral density**. The associated *Bonami-Estrade field* X^f is defined through its harmonizable representation:

$$X^f : \begin{cases} \mathbb{R}^2 & \rightarrow \\ \underline{x} & \mapsto \int_{\mathbb{R}^2} (\exp(i\underline{x} \cdot \underline{\xi}) - 1) \sqrt{f(\underline{\xi})} \tilde{W}(d\xi) \end{cases}$$

with W a Brownian measure; \tilde{W} its Fourier transform.

[A. Bonami & A. Estrade, 2003, *J. Fourier Anal. Appl.*]

Anisotropic Self-Similar Fields

Definition: Let $f \in L^1(\min(1, |\underline{\xi}|^2)d\xi)$ a **spectral density**. The associated *Bonami-Estrade field* X^f is defined through its harmonizable representation:

$$X^f : \begin{cases} \mathbb{R}^2 & \rightarrow \mathbb{R} \\ \underline{x} & \mapsto \int_{\mathbb{R}^2} (\exp(i\underline{x} \cdot \underline{\xi}) - 1) \sqrt{f(\underline{\xi})} \tilde{W}(d\xi) \end{cases}$$

with W a Brownian measure; \tilde{W} its Fourier transform.

[A. Bonami & A. Estrade, 2003, *J. Fourier Anal. Appl.*]

Spectral density encodes visual and statistical properties such as

- (an)isotropy
- preferential directions
- short or long range dependencies

The Anisotropic Fractional Brownian Field

The **anisotropic fractional Brownian field** is defined as

$$X^f(\underline{x}) = \int_{\mathbb{R}^2} (\exp(i\underline{x} \cdot \underline{\xi}) - 1) \sqrt{f(\underline{\xi})} \tilde{W}(d\xi)$$

with **spectral density** $f(\underline{\xi}) = \tau \left(\frac{\underline{\xi}}{\|\underline{\xi}\|} \right) \|\underline{\xi}\|^{-2h} \left(\frac{\underline{\xi}}{\|\underline{\xi}\|} \right)^{-2}$ with

- $\tau : \mathbb{S}_1 \rightarrow \mathbb{R}_+$ the **topothesy** function
- $h : \mathbb{S}_1 \rightarrow]0, 1[$ the **Hurst** function

Package PyAFBF for the simulation of rough anisotropic image textures

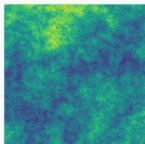
fjprichard.github.io/PyAFBF

[F. J. Richard & H. Biermé, 2011, *J. Math. Imaging Vis.*]

Particular (anisotropic) fractional Brownian fields

H -fractional Brownian field $H\text{-fBf}$: $h \equiv H$, $\tau \equiv \sigma^2/\mathcal{C}_H$ both **constant**

Field X^f



Hurst function h



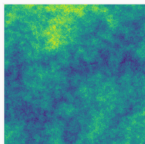
Topothesy function τ



Particular (anisotropic) fractional Brownian fields

H -fractional Brownian field $H\text{-fBf}$: $h \equiv H$, $\tau \equiv \sigma^2/\mathcal{C}_H$ both **constant**

Field X^f



Hurst function h



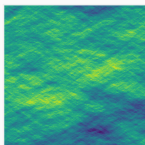
Topophesy function τ



H -anisotropic fractional Brownian field $H\text{-afBf}$: $h \equiv H$ **constant**

⇒ directional modulation of the variance of the field via τ

Field X^f



Hurst function h



Topophesy function τ

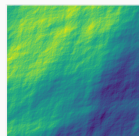
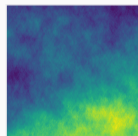
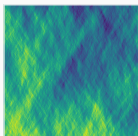


General anisotropic fractional Brownian fields

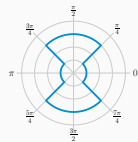
Anisotropic fractional Brownian field afBf: modulation of both

- ⇒ the variance of the field via τ
- ⇒ the decay the spectral density via h

X^f



$h(\vartheta)$



$\tau(\vartheta)$



Uniform Hölder regularity of anisotropic fields

Definition: The uniform Hölder regularity of the field X^f is H_{\min} if

$$\exists A, B > 0, \text{ such that: } \forall \|\underline{\xi}\| > A, \quad f(\underline{\xi}) \leq B \|\underline{\xi}\|^{-2H_{\min}-2}.$$

Anisotropic fractional Brownian fields have uniform Hölder regularity

$$H_{\min} = \operatorname{essinf}_{\vartheta \in \mathbb{S}_1} h(\vartheta)$$

From **Kolmogorov-Chenov theorem**

- H -(isotropic) fractional Brownian field B_H : $H_{\min} = H$
- H -anisotropic fractional Brownian field B_H : $H_{\min} = H$

Same uniform Hölder regularity H_{\min} for H -fBf and H -afBf.

[S. Cohen & J. Istas, 2013, Springer]

Analysis of anisotropic fractal textures

- Directional increments & Radon transform: [H. Biermé et al., 2008,
ESAIM: Proba. Stat.]

$$(\forall (\vartheta, t) \in \mathbb{S}^1 \times \mathbb{R}) \quad \mathcal{R}_\rho X(\vartheta, t) = \int_{\mathbb{R}} X(s\vartheta^\perp + t\vartheta) \rho(s) \, ds$$

windowed Radon transform with ρ Schwartz class

Analysis of anisotropic fractal textures

- Directional increments & Radon transform: [H. Biermé et al., 2008, *ESAIM: Proba. Stat.*]

$$(\forall (\vartheta, t) \in \mathbb{S}^1 \times \mathbb{R}) \quad \mathcal{R}_\rho X(\vartheta, t) = \int_{\mathbb{R}} X(s\vartheta^\perp + t\vartheta) \rho(s) \, ds$$

windowed Radon transform with ρ Schwartz class

- X-let and scattering transform: [S. Mallat, 2008, *Acad. Press*; J. Bruna, 2013, *PhD thesis*] kymat.io

scattering coefficients of order n : $|||X * \psi_{\theta_1, j_1} | * \psi_{\theta_2, j_2} | \dots * \psi_{\theta_n, j_n} | * \varphi_J$

Analysis of anisotropic fractal textures

- Directional increments & Radon transform: [H. Biermé et al., 2008, *ESAIM: Proba. Stat.*]

$$(\forall (\vartheta, t) \in \mathbb{S}^1 \times \mathbb{R}) \quad \mathcal{R}_\rho X(\vartheta, t) = \int_{\mathbb{R}} X(s\vartheta^\perp + t\vartheta)\rho(s) \, ds$$

windowed Radon transform with ρ Schwartz class

- X-let and scattering transform: [S. Mallat, 2008, *Acad. Press*; J. Bruna, 2013, *PhD thesis*] [kymat.io](#)

scattering coefficients of order n : $|||X * \psi_{\theta_1, j_1} | * \psi_{\theta_2, j_2} | \dots * \psi_{\theta_n, j_n} | * \varphi_J$

- Monogenic Images [H. Biermé et al., 2024, *Preprint*]

$$\mathcal{M}X(w) = (\langle X, w \rangle, \langle \mathcal{R}_1 X, w \rangle, \langle \mathcal{R}_2 X, w \rangle)$$

$$\mathcal{R}_k w(\underline{x}) = \frac{1}{2\pi} \lim_{\varepsilon \rightarrow 0} \int_{\mathbb{R}^2 \setminus B(0, \varepsilon)} \frac{x_k - y_k}{\|\underline{x} - \underline{y}\|^3} w(\underline{y}) \, d\underline{y}$$
 Riesz transform

Wavelet analysis of anisotropic fractal textures

Multiband complex wavelet transform

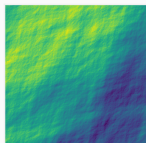
$(\psi^{(1)}, \dots, \psi^{(B)})$ B complex mother wavelets: $\psi^{(b)} : \mathbb{R}^2 \rightarrow \mathbb{C}$ such that

$$\psi^{(b)} = \psi^{(0)} (\mathcal{R}_{\vartheta_b}^\top \cdot) \quad \tilde{\psi}^{(b)} = \tilde{\psi}^{(0)} (\mathcal{R}_{\vartheta_b}^\top \cdot)$$

for $\psi^{(0)}$ a frequency-direction selective complex mother wavelet;

multiband wavelet coefficients: $\zeta_{j,\underline{k}}^{(b)} = \langle X, \psi_{j,\underline{k}}^{(b)} \rangle$

Field X^f



Hurst function h

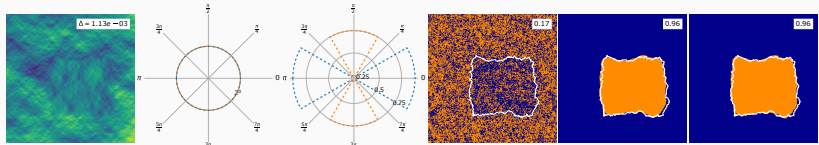


Topophesy function τ



Segmentation of piecewise homogeneous anisotropic textures

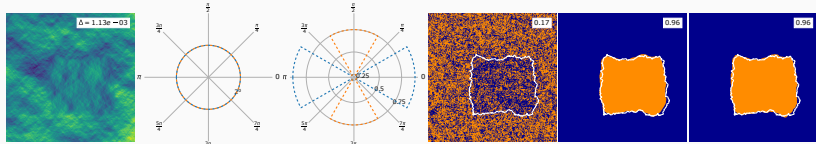
Synthesis *M*-class piecewise homogeneous Gaussian Bonami-Estrade field



- $M = 2$ textures: background vs. central rectangle
- **same** topography
- **different** Hurst functions

Segmentation of piecewise homogeneous anisotropic textures

Synthesis M -class piecewise homogeneous Gaussian Bonami-Estrade field



- $M = 2$ textures: background vs. central rectangle
- **same** topography
- **different** Hurst functions

Segmentation: requires accurate contour localization

Non-decimated Dual Tree Complex Wavelet Transform $\zeta_{j,\underline{n}}^{(b)}$

Theorem Let X^f a piecewise homogeneous Gaussian Bonami-Estrade field.

The multiband wavelet coefficients $\zeta_{j,\underline{n}}^{(b)} = \langle X^f, \psi_{j,\underline{n}}^{(b)} \rangle$ satisfy

$$\zeta_{j,\underline{n}}^{(b)} \sim \mathcal{N} \left(0, \left(\sigma_{j,\underline{n}}^{(b)} \right)^2 \right) \quad \text{with} \quad \left(\sigma_{j,\underline{n}}^{(b)} \right)^2 \sim \mathcal{V}(\tau, h, \psi^{(b)}) 2^{j2H(h, \psi^{(b)})}$$

Anisotropic texture segmentation: take home messages

► Non-decimated multiband wavelet coefficients

- behaves locally approximately as **power laws**
- local scaling exponents depending on **Hurst function**
- local intercept providing information about **topothesy function**

Anisotropic texture segmentation: take home messages

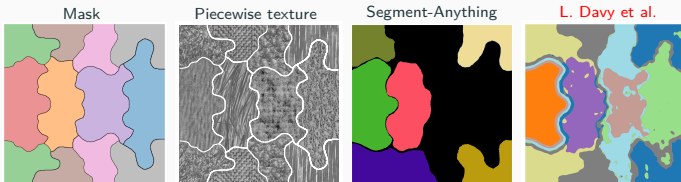
► Non-decimated multiband wavelet coefficients

- behaves locally approximately as **power laws**
- local scaling exponents depending on **Hurst function**
- local intercept providing information about **topothesy function**

► Regularized estimates of scaling exponents and intercept

- approximate **power-law** model for multiband wavelet coefficients
- penalization enforcing pixel-wise spatial **piecewise constancy**
- excellent segmentation performance in **various configurations**

Natural textures characterized by joint fractal and anisotropy properties



[L. Davy et al., 2023, ICASSP; L. Davy et al., 2024, EUSIPCO;

L. Davy et al., 2025, Preprint]